Since January 2020 Elsevier has created a COVID-19 resource centre with free information in English and Mandarin on the novel coronavirus COVID-19. The COVID-19 resource centre is hosted on Elsevier Connect, the company's public news and information website.

Ceramics International 48 (2022) 34148–34168

Contents lists available at ScienceDirect

Ceramics International

journal homepage: www.elsevier.com/locate/ceramint

Review article

The mechanism of metal-based antibacterial materials and the progress of food packaging applications: A review

Xiaotong Yang [a,1], Qingjun Yu [a,b,1], Wei Gao [a], Xiaoning Tang [c], Honghong Yi [a,b], Xiaolong Tang [a,b,*]

[a] Department of Environmental Science and Engineering, School of Energy and Environmental Engineering, University of Science and Technology Beijing, Beijing, 100083, China
[b] Beijing Key Laboratory of Resource-oriented Treatment of Industrial Pollutants, Beijing, 100083, China
[c] Faculty of Chemical Engineering, Kunming University of Science and Technology, Kunming, 650500, Yunnan, China

ARTICLE INFO

Keywords:
Antibacterial mechanism
Metal
Carrier
Coating method
Food packaging

ABSTRACT

Food packages have been detected carrying novel coronavirus in multi-locations since the outbreak of COVID-19, causing major concern in the field of food safety. Metal-based supported materials are widely used for sterilization due to their excellent antibacterial properties as well as low biological resistance. As the principal part of antibacterial materials, the active component, commonly referred to Ag, Cu, Zn, etc., plays the main role in inhibiting and killing pathogenic microorganisms by destroying the structure of cells. As another composition of metal-based antibacterial materials, the carrier could support and disperse the active component, which on one hand, could effectively decrease the usage amount of active component, on the other hand, could be processed into various forms to broaden the application range of antibacterial materials. Different from other metal-based antibacterial reviews, in order to highlight the detailed function of various carriers, we divided the carriers into biocompatible and adsorptable types and discussed their different antibacterial effects. Moreover, a novel substitution antibacterial mechanism was proposed. The coating and shaping techniques of metal-based antibacterial materials as well as their applications in food storage at ambient and low temperatures are also comprehensively summarized. This review aims to provide a theoretical basis and reference for researchers in this field to develop new metal-based antibacterial materials.

1. Introduction

Since the beginning of the 21st century, the successive occurrence of global epidemics caused by pathogenic microorganisms such as SARS, H1N1, MERS, and COVID-19, etc., has seriously threatened the development of the national economy and people's life safety. Therefore, it is especially important to enhance antibacterial awareness and eliminate pathogenic microorganisms. Antibacterial materials are bactericidal and antibacterial, with large-scale applications dating back to World War II, when the German used uniforms soaked with ammonium cationic antibacterial agents to reduce infection among wounded soldiers [1]. Furthermore, the mass infection of O-157 bacteria in Japan in 1996 again prompted antibacterial materials to the public eye [2]. However, new research shows that antibacterial resistance is a major roadblock for fighting against pathogenic microorganisms [3]. In 2019, 1.27 million individuals died directly from antibacterial resistance infections, while 4.95 million deaths were indirectly related with the infections, far more than the deaths caused by AIDS or malaria [3]. Therefore, it is crucial to develop novel and highly efficient antibacterial materials.

Antibacterial materials can be divided into natural antibacterial materials, organic antibacterial materials, and inorganic antibacterial materials according to the types of antibacterial active components. Natural antibacterial materials have high biocompatibility, however, little attention was paid due to their limited supplies and antibacterial properties. Despite possessing better antibacterial properties and mature preparation processes, organic antibacterial materials are noxious and prone to bacterial resistance. By contrast, antibacterial materials based on metals have become caused more and more attention as an efficient

* Corresponding author. Department of Environmental Science and Engineering, School of Energy and Environmental Engineering, University of Science and Technology Beijing, Beijing, 100083, China.
E-mail address: txiaolong@126.com (X. Tang).
[1] These authors contributed equally.

https://doi.org/10.1016/j.ceramint.2022.08.249
Received 9 July 2022; Received in revised form 10 August 2022; Accepted 23 August 2022
Available online 27 August 2022

measure to cure antibacterial resistant infections because of its advantages of both safety and resistance. Thereby, in this review, the antibacterial mechanism of metal-based antibacterial materials was systematically analyzed and summarized. In addition, a new antibacterial mechanism—substitution antibacterial type—was proposed. Besides, the synergistic effect of multiple metal active components, as well as the impact of different carriers on the antibacterial effect, is summarized in detail for better understand. Different from the previous classification of antibacterial carriers, carriers were classified into biocompatible and adsorptable types based on their functionality. Furthermore, the technology of antibacterial coating and its application in food preservation are discussed. Finally, the migration behavior and toxicity of metal antibacterial active components in food packaging were analyzed.

2. Antibacterial mechanisms

Clarifying the antibacterial mechanism is an important step to optimize and improve the performance of metal-based antibacterial materials. Despite many investigators have reported their discoveries of antibacterial mechanisms, it is still hard to get a general conclusion, especially for some active metal with unique antibacterial properties, the mechanism is often complicated and even involve multiple actions. Here, according to the action ways of antibacterial active component, the antibacterial mechanism could be divided into the following four categories: contact antibacterial type, dissolution antibacterial type, oxidation antibacterial type, and substitution antibacterial type, and the mechanisms are shown in Fig. 1.

2.1. Contact antibacterial type

The contact antibacterial type refers to the direct action of the antibacterial active component on the cell wall (membrane), affecting its normal physiological function by disrupting the integrity of the internal structure and finally resulting in the efflux of cell contents, which leads to cell death. Electrostatic attraction has been viewed as the major cause for the positively charged active components adsorbed on the cell wall (membrane) [4]. This is mostly because bacterial cells contain too many carboxyl and phosphate groups, resulting in a negative total cell surface charge when these groups dissociate [5]. Therefore, the cell tends to attract the surrounding positively charged antibacterial active components to the membrane surface. Xing et al. investigated the electrostatic interaction between gold nanoparticles (AuNPs) with positive charge modification and phospholipid membranes. To replicate variations in electrostatic attraction, vesicles formed by different phospholipid molecules were used to simulate bacterial cell membranes. As shown in Fig. 2, the electrostatic attraction is greatest when AuNPs contact the surface of lipid vesicles but rapidly declines as AuNPs reach the vesicles [6]. In contact with bacterial cell membranes, antibacterial active components can react with the substances in the membranes, forming 'pits' and changing the morphologies of bacteria [7]. The findings of Liu et also demonstrated that the antibacterial active component (TiO_2), can effectively destroy the cell wall (membrane) of

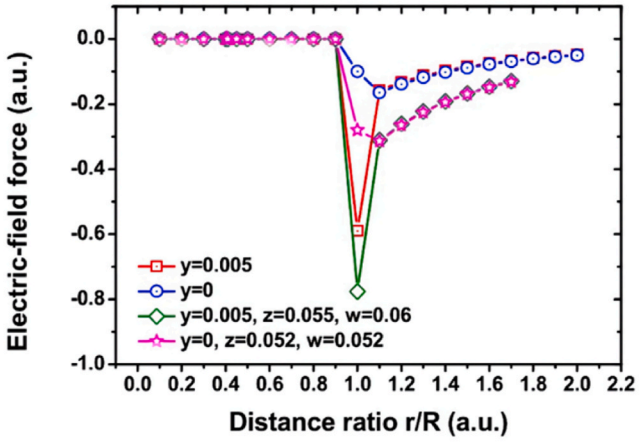

Fig. 2. Simulation of electrostatic interaction of vesicles with positively charged AuNP.

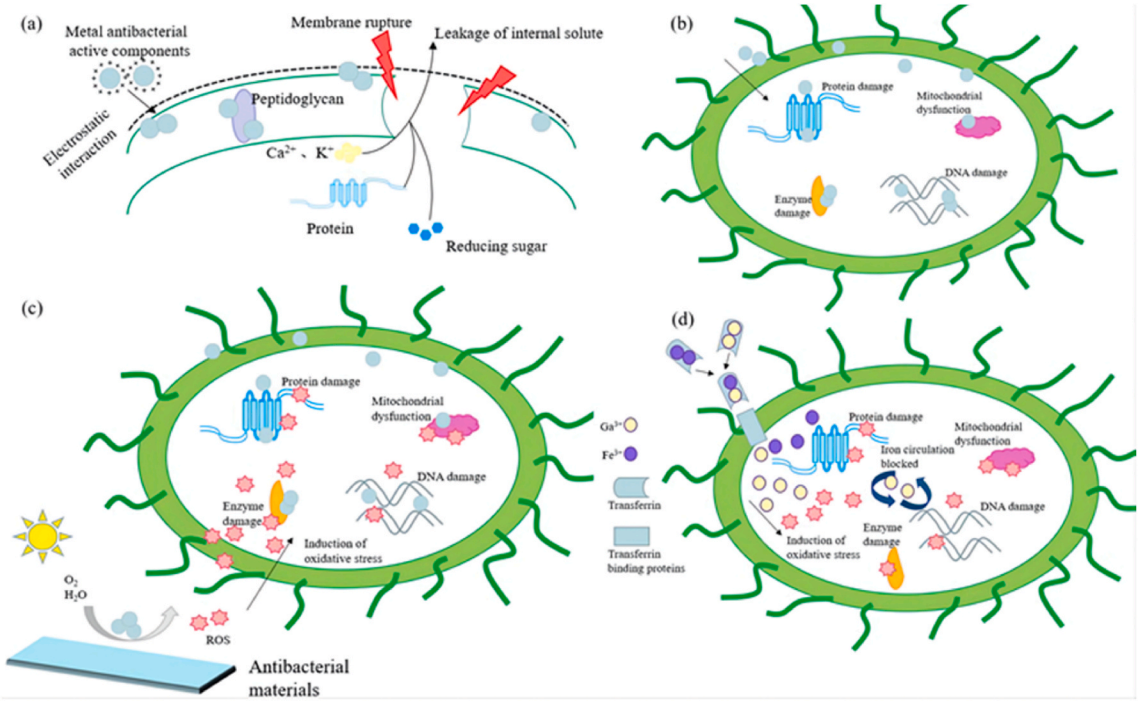

Fig. 1. Antibacterial mechanism of metal based materials (a) Contact antibacterial type; (b) Dissolution antibacterial type; (c) Oxidation antibacterial type; (d) Substitution antibacterial type.

bacteria, as illustrated in Fig. 3. The surface of natural *E. coli* was almost intact and maintained a rod-like shape, with regular folds at nanoscale resolution. When was treated with TiO_2 solution or UV light, the morphology of *E. coli* altered dramatically, with grooved cracks on the surface and swollen of cell ends, as well as shorter cell length. However, the sample that was treated with both TiO_2 and UV had a large and deep hole covering more than half of the surface area compared to samples B and D. Moreover, when the cell membrane was disrupted, the concentrations of Ca^{2+} and Mg^{2+} in the media increased, as did the fluorescence polarization of DPH. Following cell membrane injury, the permeability of the *E. coli* membrane increases while the fluidity decreases, affecting the exchange of substances between the cell and the outside [8]. Besides releasing intracellular ions, the damage of membranes will also cause the leak of substances necessary for cell growth, i.e., proteins, reducing sugars, etc. Wang et al. prepared silver nanoparticles (AgNPs) with an average particle size of 31.2 nm using citrate reduced Ag^{+} and tested their antibacterial activity against *Cronobacter sakazakii* strains. After 2 h of treatment with 200 mg/L AgNPs, the cell membrane was found to have lost its integrity. A further test was performed to determine the bacterial cultures' protein and sugar content variation with AgNPs addition. As shown in Fig. 4, all four AgNPs-treated strains displayed evident sugar and protein leakage, confirming that AgNPs induce cell death by disrupting the structure of cell membranes, causing cell contents to flow out [9].

Many researches have been made to study the detailed mechanism of cell wall (membrane) destroyed by antibacterial active component and two types of damage mechanism were obtained. One is that the cell wall (membrane) is ruptured by mechanical damage from the rough edge of the antibacterial active component. The other is that the antibacterial active component interacts with materials in the cell wall (membrane), such as peptidoglycan and –SH in proteins, to disrupt its structure, leading to the cell demise. According to Gilbertson et al., copper oxide nanosheets have an irregular edge structure that enhances physical collisions with the cell wall, resulting in more damage to it [10]. Similarly, Padmavathy et al. revealed surface defects in the 450–550 nm region of ZnO by photoluminescence (PL) spectroscopy, making it have rough edges and an inhomogeneous surface structure. This surface roughness can lead to mechanical damage to *E. coli* cell membranes [11]. However, mechanical damage is not considered to be the main cause of cell wall (membrane) damage because force majeure factors such as collision and friction could also occur during antibacterial assays, which will result in damage to cells. Therefore, the action of the antibacterial active components on substances in the membrane is of greater interest. Ansari et al. investigated the interaction between Al_2O_3 nanoparticles and *E. coli* cell membrane biomolecules. Infrared (IR) spectral and reflectance/Fourier transform infrared (ATR-FTIR) results of the interaction between Al_2O_3 and lipopolysaccharide (LPS) showed that LPS and L-α- Phosphatidyl-ethanolamine (PE) could interact with Al_2O_3-NP. Compared with *E. coli* without Al_2O_3-

NP treatment, PE in Al_2O_3-treated *E. coli* showed a disordered state. The structural changes of phospholipids induced by Al_2O_3-NP was viewed to be able to lead to cell membrane disruption and cell leakage [12]. Mirzajani et al. released muramic acid (MA) into the medium while monitoring AgNP-treated *Staphylococcus aureus* (*S. aureus*) using circular dichroism(CD) to reveal changes in peptidoglycan (PGN). The data showed that in the 210–220 nm region, the correlation of the samples treated with AgNPs was opposite to that of pure PGN, and the samples changed after 30 min and 3 h of treatment. This indicated that AgNPs changed the secondary structure (α-helix and hydrogen bond) of the PGN. To further investigate the effect of AgNPs on PGN glycan strands, samples were examined by gas chromatography-tandem mass spectrometry (GC-MS^n). It was found the concentration of MA increased in the medium of AgNP-treated samples, confirming the strong interaction between AgNPs and PGN led to the breakage of PGN glycan strands. Moreover, this strong interaction causes the leakage of intracellular amino sugar particles like MA, resulting in the continuous enlargement of pits generated in the cell wall and finally, the rupture contributed to cell death [13].

2.2. Dissolution antibacterial type

Dissolution antibacterial type means the antibacterial active component released from the metal-based antibacterial materials in the from of ion or nanoparticle enters the interior of the cell by going through the cell wall (membrane) and react with intracellular proteins, nucleic acids, and other substances, inhibiting the normal life activities of bacteria and causing death. With the development of nanotechnology, many new metal nanometer antibacterial materials have been obtained, among which nanomaterials were believed to contact with bacteria and other microorganisms closely due to the large specific surface area provided by small sized metal particles, which was speculated to be 'particle-effect'. To verify whether the antibacterial effect of AgNPs caused by the specificity of nanoparticles, Xiu et al. conducted experiments under anaerobic conditions to eliminate the possibility of silver ion (Ag^{+}) release. The medium was free of chloride, sulfide, phosphate, and other substances affecting the bioavailability of silver, while *E. coli* strains showing equal sensitivity to Ag^{+} in aerobic and anaerobic conditions were selected for the antibacterial test. It was showed that the

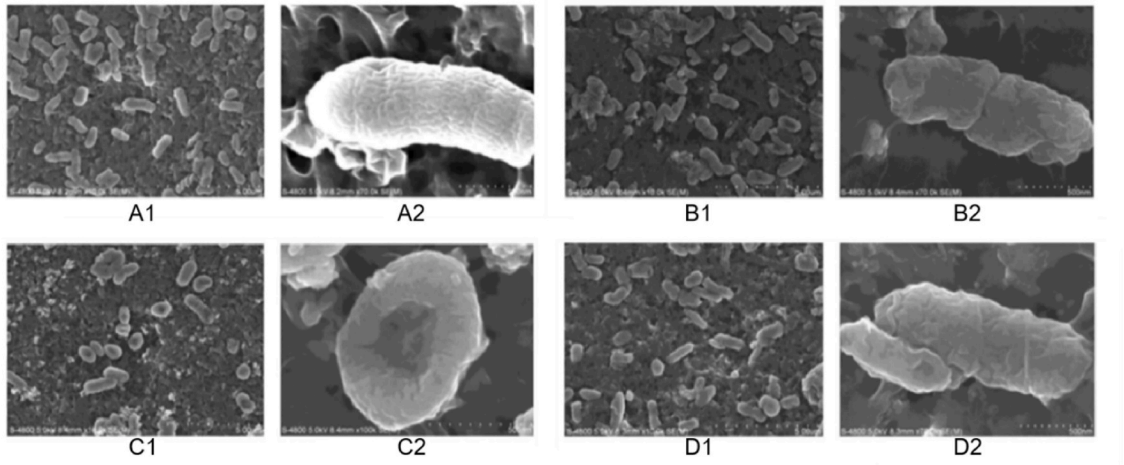

Fig. 3. SEM images of A (the control): the native cells in PBS with shaking for 1 h; B: the cells in PBS in the presence of 0.35 mg/mL TiO_2 solution under natural light with shaking for 1 h; C: the cells in PBS in the presence of 0.35 mg/mL TiO_2 solution under 500W UV light (mainly 365 nm) for 1 h; D: the cells in PBS with 500W UV (mainly 365 nm) light for 1 h.

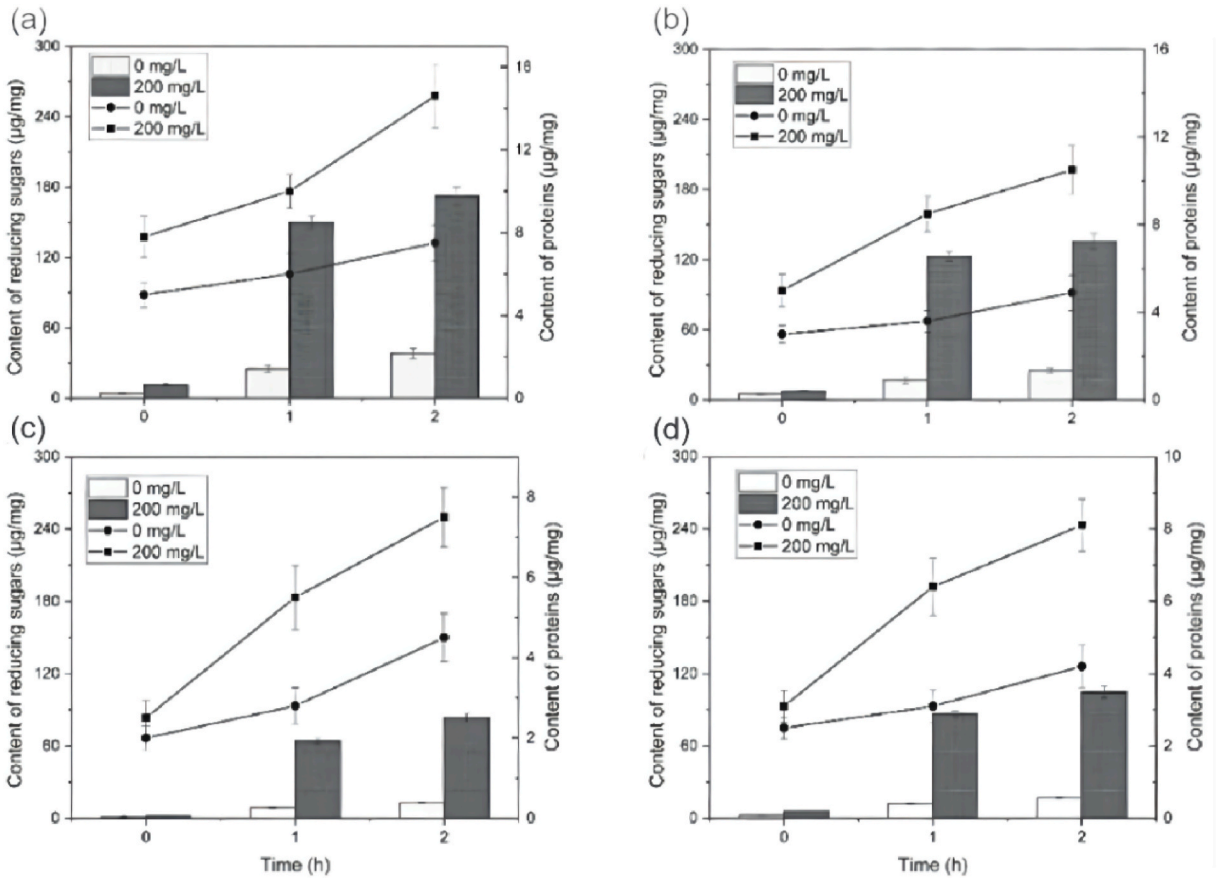

Fig. 4. Leakage of reducing sugars (bars) and proteins (—●—) for 4 Cronobacter sakazakii strains without (0 mg/L) or with treatment of silver nanoparticles at a final concentration of 200 mg/L: (a) ATCC 29544T; (b) ATCC BAA894; (c) ATCC 29004; (d) ATCC 12868. Error bars represent the SD of data from 3 repetitive experiments.

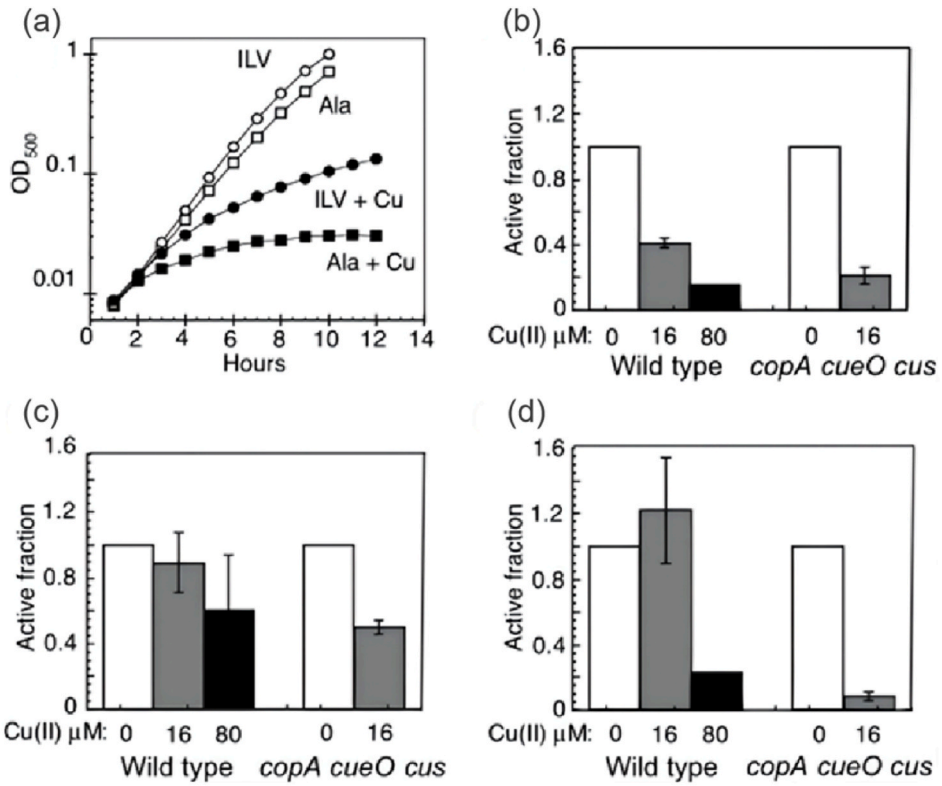

Fig. 5. Copper damages iron-sulfur-cluster dehydratases. (A) LEM33 (*copA cueO cusCFBA*) was grown at 37°C in aerobic glucose medium with 1.5 mM alanine (*Ala*) (squares) or 0.5 mM each of isoleucine (*I*), leucine (*L*), and valine (*V*) (circles), and $CuSO_4$ was added to 0 M (open symbols) or 10 M (closed symbols). The data are a representative of 3 independent experiments. (B–D) W3110 (WT) and LEM33 (*copA cueO cusCFBA*) were grown aerobically to an OD_{500} of 0.1, then challenged with 0 M (open bars), 16 M (gray bars), or 80 M $CuSO_4$ (black bars) for 30 min. (B and C) Cells were grown in glucose/alanine, and IPMI (B) and fumarase (C) activities were measured. (D) Cells were grown aerobically in gluconate medium supplemented with 1.5 mM alanine, and 6-phosphogluconate activity was measured. (B–D) Data are the average of 3 independent experiments, and the error bars represent SD. (B) WT cells exposed to 80 M Cu had IPMI activities below the detection limit (15%).

minimum lethal concentration (MLC) of 5 and 11 nm AgNPs prepared under anaerobic conditions against *E. coli* were 158 mg/L and 195 mg/L respectively, which were 6224 and 7665 times higher than the MLC of Ag^+ (0.025 mg/L), demonstrating that the AgNPs have no effect on the biological activity of microorganisms. Nevertheless, the antibacterial activity would be enhanced after being subjected to aerobic conditions for 6 h and this is probably because the oxidation of the crystal nucleus and release of Ag^+ occurring under aerobic conditions conferring the antibacterial ability of AgNPs. AgNPs, despite of their 'particle effect', cannot be significantly antibacterial; however, their large surface area makes it easier for pathogenic microorganisms to contact with them, resulting in effective delivery of Ag^+ into the cell, where it reacts with intracellular material and causes cellular inactivation [14].

It was also reported that antibacterial active components entering the cell interior can coagulate proteins by reacting with their sulfhydryl groups, inhibit the activity of respiratory enzymes and impede DNA replication, leading to dysfunctional and metabolic impairment of bacteria [15,16]. Macomber et al. used an E. coli mutant (*copA cueO cusCFBA*) lacking the copper homeostatic system to identify the main targets of copper action. As shown in Fig. 5, the *copA cueO cusCFBA* mutant failed to grow in 10 μM copper medium but recovered with the addition of branched-chain amino acids, indicating that copper ions hindered its biosynthesis. The cellular activity of the wild-type strain and the *copA cueO cusCFBA* mutant strain were reduced by 60% and 80%, respectively, after 30 min of exposure to 16 μM copper. Furthermore, ferredoxin A and 6-phosphogluconate dehydratase, both of which use iron-sulfur clusters, exhibit decreased activity. These results demonstrated that long-term exposure to copper disrupts enzyme synthesis, reduces the enzyme activity, and interferes with amino acid synthesis [17]. Additionally, Kang et al. analyzed the proteomics of *E. coli* and *S. aureus* treated with Ag^+ and identified five proteins with reduced expression after two-dimensional electrophoresis and peptide mass fingerprinting by NCBI and Swiss-Prot databases [18]. The integrity of DNA is vital for cellular growth and reproduction, and its loss can lead to gene mutation or cell death. Abbas et al. measured exoA gene expression by real-time polymerase chain reaction in *Pseudomonas aeruginosa*(*P. aeruginosa*) treated with AgNPs. The AgNPs-treated samples showed amplification after $4C_T$ (cyclic cycle), and delayed amplification of the exoA gene. Especially, when the AgNPs dosage was 50 ppm, the exoA gene expression decreased significantly. The results of this experiment demonstrated that AgNPs could cause DNA damage to bacteria [19]. Similarly, the results of Singh's experiments confirmed that ZnO-NP caused severe damage to the DNA of *Deinococcus radiodurans*. The F values (ratio of double-stranded DNA to total DNA) of cells treated with different concentrations of ZnO-NP at 1, 10, 20, 40, and 80 μg/mL were decreased to 0.90, 0.79, 0.73, 0.60, and 0.25 fold, respectively, compared with the sample untreated by alkaline unwinding assay. The 'F' values were inversely proportional to DNA damage, thus indicating that ZnO-NP caused DNA damage to the cells [20].

2.3. Oxidation antibacterial type

By using antibacterial active components, the oxidative antibacterial type contribute to the increase of intracellular reactive oxygen species (ROS), inducing oxidative stress response in cells, which will result in the destruction of proteins, genetic material, enzymes, and other critical substances required for the growth and metabolism of organisms, thereby leading to cell death. ROS are essential for maintaining cell survival and transmitting cellular signals. The mechanism of ROS generated by various antibacterial active components are mainly divided into two different types. (1) Electrons are supplied to molecular oxygen in the cell, generating free radical superoxide anion (O_2^-), hydrogen peroxide (H_2O_2), hydroxyl radical (OH^-), etc., and inducing an oxidative stress reaction in the cell. Ahmed examined the effect of ROS produced by two AgNPs (Q-AgNPs、YPE-AgNPs) prepared from quercetin extract and yellow bell pepper extract, on bacterial growth. The experimental results are shown in Fig. 6. In contrast to samples without AgNPs, Confocal Laser Scanning Microscope (CLSM) images of samples treated with different concentrations of AgNPs showed different brightness of green fluorescence. In addition, the fluorescence intensity of 2',7'-dichlorofluorescein (DCF) was quantified. It was revealed that Q-AgNPs could produce more ROS compared to YPE-AgNPs, and 9%–31% more O_2^- was produced by Q-AgNPs under light conditions (10–50 μg/ml) than under dark conditions [21]. (2) Some antibacterial active components with photocatalytic properties could be activated by ultraviolet or visible light, and react with oxidizing substances (i.e., oxygen and water) adsorbed on the surface of the material to generate numerous oxidative radicals. When entering cells, oxidative stress caused by oxidative radicals will occur. ZnO and TiO_2 are typical antibacterial active components that use the photocatalytic generation of reactive oxygen species to kill microorganisms. Photocatalytic antibacterial active components will be activated under light irradiation with energy higher than their forbidden band widths. Electrons in the valence band are excited to leap, leaving electron-hole pairs to react with oxygen and water in the surrounding environment, producing oxidation-active substances [22–24].

The antibacterial active component induces oxidative stress in cells by generating ROS. Oxidative stress is an imbalance between the production and degradation of intracellular ROS, leading to damage of cellular components, lipid peroxidation, protein oxidation, reduced enzyme activity, and DNA damage. Quinteros et al. investigated the mechanism of AgNPs interacting with on *S. aureus*, *E. coli*, and *P. aeruginosa*. varying degrees of elevated reactive oxygen species content were found in bacterial cells. The oxidation degree of these three macromolecules, such as DNA, lipids, and proteins, was increased by 60% compared to the control group without nanoparticles, implying that oxidative stress is generated through macromolecular oxidation at the DNA, lipid, and protein levels [25]. The findings of Piao et al. also confirmed that AgNPs induce apoptosis through DNA breakage, lipid peroxidation, and protein carbonylation caused by oxidative stress. Furthermore, AgNPs was also found to cause mitochondrial damage by disrupting mitochondrial membrane potential and regulating the expression of genes (Bax and Bcl-2) that control mitochondrial membrane pores [26].

2.4. Substitution antibacterial type

Substitution antibacterial type refers to the antibacterial element have certain structural similarities with the nutrient element necessary for bacterial growth and reproduction. As a result, the antibacterial element that enters the cell interior is difficult to be recognized by the bacterial biological system, which consequently replaces the nutrient element causing damage to the normal physiological function of the cell. Gallium ion (Ga^{3+}) and iron ion (Fe^{3+}) shared similar values of octahedral ionic radius, tetrahedral ionic radius, electron affinity, and electronegativity, making their similar biochemistry, especially in protein and chelate binding [27]. These characteristics make it impossible for bacterial biological systems to completely distinguish between Ga^{3+} and Fe^{3+}. As iron is an essential nutrient element for metabolism, the replacement of Fe^{3+} by Ga^{3+} can effectively prohibit the normal metabolic activities of bacteria [28]. To clarify the biological inhibition mechanism of Ga, Garcia et al. sequenced the genome of gallium nitrate resistant spontaneously mutated *P. aeruginosa* and found that the mutated genes were involved in cell division, iron carrier transport system, DNA repair, amino acid, and lipid metabolism, confirming the existence of multiple gallium action targets in bacterial cells [29]. Antunes et al. selected *Acinetobacter baumannii* (*A. baumannii*) possessing multiple iron uptake systems to test the effect of Ga on iron metabolic pathways. It was discovered that the addition of 50 μM Fe^{3+} eliminated the activity of 128 μM $Ga(NO_3)_3$, further confirming that the antibacterial mechanism of $Ga(NO_3)_3$ involves the disruption of iron metabolism within the bacteria [30]. Some other research also showed that

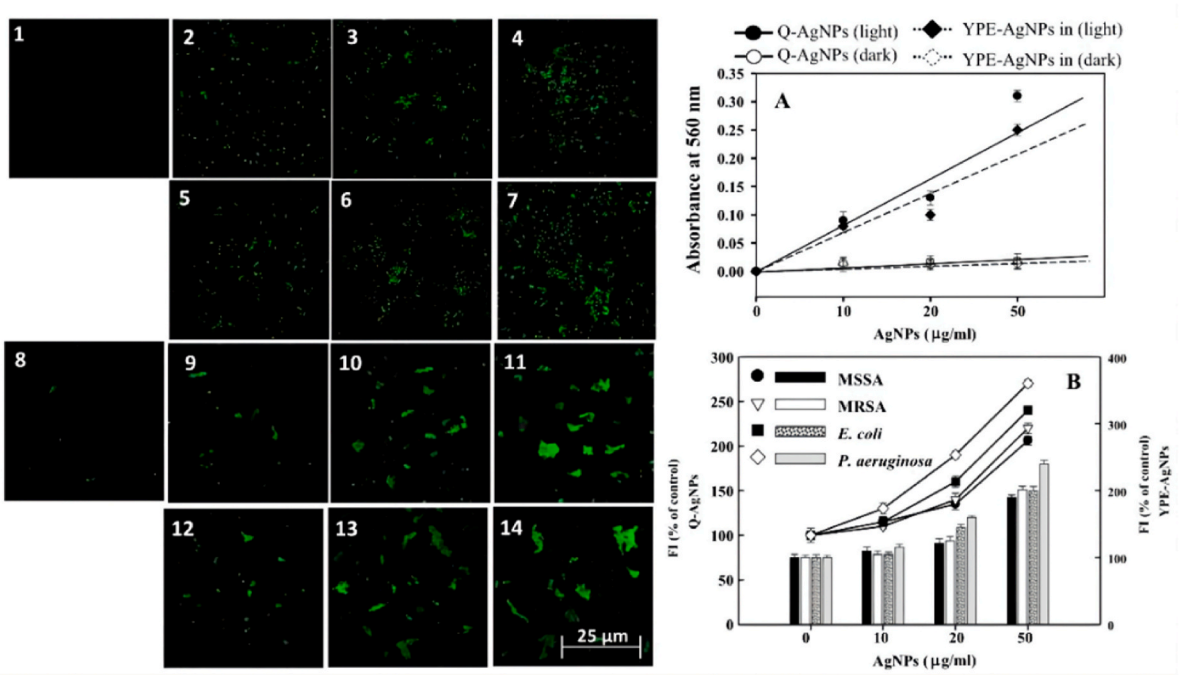

Fig. 6. YPE-AgNPS and Q-AgNPs induced ROS and superoxide generation. CLSM images (1–14) show the ROS production in *P. aeruginosa* and MRSA; untreated cells of *P.aeruginosa* (1), *P. aeruginosa* + 10 μg/ml YPE-AgNPs (2), *P. aeruginosa* + 20 μg/ml YPE-AgNPs (3), *P. aeruginosa* + 50 μg/ml YPE-AgNPs (4), *P. aeruginosa* + 10 μg/ml Q-AgNPs (5), *P. aeruginosa* + 20 μg/ml Q-AgNPs (6), *P. aeruginosa* + 50 μg/ml Q-AgNPs (7), Untreated cells of MRSA (8), MRSA + 10 μg/ml YPE-AgNPs (9), MRSA + 20 μg/ml YPE-AgNPs (10),MRSA + 50 μg/ml YPE-AgNPs (11), MRSA + 10 μg/ml Q-AgNPs (12), MRSA + 20 μg/ml Q-AgNPs (13), and MRSA + 50 μg/ml Q-AgNPs (14). Panel A shows in vitro superoxide anions generation by YPE-AgNPs and Q-AgNPs under light and dark conditions. Panel B represents the percent increase in DCF fluorescence in MRSA, MSSA, E. coli, and *P. aeruginosa* by Q-AgNPs (line curves) and YPE-AgNPs (histograms).

Ga could not only bind to iron carriers but also could combine with transferrin and lactoferrin to form a complex delivered into bacteria [31]. Thus, exogenous gallium can participate in bacterial metabolism to achieve antibacterial purposes. Besides, the inhibitory effect of Ga^{3+} on bacteria and other pathogenic microorganisms can be reflected in disrupting bacterial cell membranes [32], reducing iron-dependent enzyme activity [33], preventing DNA synthesis [34], and generating oxidative stress [35].

In addition to Ga^{3+}, cerium ions(Ce^{4+}, Ce^{3+}) also could compete with intracellular calcium ions. Ciobanu et al. investigated the antibacterial effect of hydroxyapatite (HAp) nanopowders containing Ce against *E. coli* and *S. aureus*, and the experimental results are given in Fig. 7. The antibacterial effect against *E. coli* and *S. aureus* increased with the Ce concentration addition in HAp [36]. Correspondingly, the Ca^{2+}replacement theory was proposed for Ce inhibiting bacterial growth [37] except for the direct adsorption on the cell membrane to disrupt its structure [38] and induce oxidative stress in cells to interfere with DNA and protein synthesis. This theory suggests that Ce^{4+}, Ce^{3+} possesses the similar ionic radii to Ca^{2+} and hence, are capable of occupying the original calcium sites in the cell [39]. In addition, as a hard acid ion that is not easily deformed by polarization, cerium ion has a stronger coordination ability with oxygen, nitrogen, and sulfur than calcium ion [40]. As a result, it can cause the lack of Ca^{2+} in the cell to affect the metabolic activities of bacteria aimed at antibacterial purposes. However, few reports cover the biological antibacterial properties and applications of cerium, and the mechanism of calcium ion substitution in more detail needs to be further clarified.

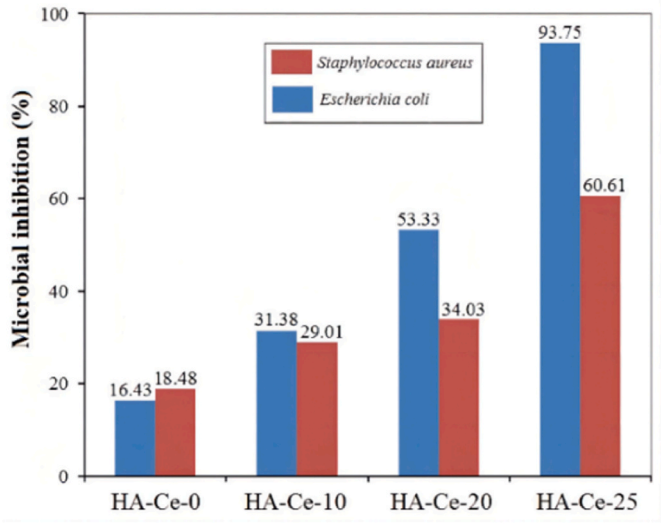

Fig. 7. Samples inhibition results against *Escherichia coli* and *Staphylococcus aureus*.

3. Antibacterial active components

As the main component of antibacterial materials, the properties and structure of active components play a critical role in affecting the antibacterial properties. There are many metals with antibacterial functions in nature, such as Ag, Cu, Zn, Fe, Mn, Al, Mg, Sr, Co, Ce, Ni, Sn, Zr, Cd, Ba. However, considering factors of economy, safety, and antibacterial efficiency, the currently applied antibacterial metals are mainly Ag, Cu, and Zn [41]. The antibacterial properties of these three common types of metals are summarized in Table 1.

Recently, considerable progress has been made in the development and application of single-metal antibacterial materials. Single-metal antibacterial materials do have inherent defects. For example, Ag^{+} is easily oxidized, thereby reducing its antibacterial performance. Additionally, copper ions containing color will interfere with the coloring of antibacterial materials. To further improve the antibacterial effect of existing metal-baesd antibacterial materials and compensate for the

Table 1
Antibacterial effect of common forms of Ag, Cu, and Zn.

Antibacterial active components	Zone of inhibition(mm)/MIC(μg/ml)			References
	E. coli	S. aureus	P. aeruginosa	
silver nanoparticles	14.2/8.3	10/33.1	19.5/8.3	[42]
Silver ion	7.3/12	8.3/20	9.8/12	[43]
Copper nanoparticles	12/<100	18/<50	15/<100	[44]
Native copper	8/ 100~200	12/ 100~200	10/ 100~200	[44]
Copper oxide nanomaterial	25.33/-	28.66/3.13	25.66/1.56	[45,46]
Zinc oxide nanomaterial	22/172.5	25/86.25	–	[47,48]

shortcomings of single-metal antibacterial materials, researchers have turned their attention to developing composite materials containing multiple antibacterial active components. Through compounding and doping to improve the physical and chemical properties of materials, synergistic effects between antibacterial components can be achieved, enhancing antibacterial effects. According to the different antibacterial active components added, the multi-metal antibacterial active components can be divided into metal composite type, photocatalytic composite type and rareearth activated type.

3.1. Metal composite type

Metal composite type means recombination of two or more antibacterial metals to enhances the overall antibacterial effect according to the synergistic effect of different metals. Zhu et al. synthesized Ag–MgO nanocomposites by loading small-sized AgNPs on the surface of MgO-NPs and applied for bacterial inactivation. The XRD patterns showed that the diffraction peaks of MgO in Ag–MgO nanocomposites were shifted to a higher angle compared to pure MgO nanocomposites, indicating an interaction between MgO and Ag rather than a simple physical mixing. Compared with pure MgO and AgNPs, Ag–MgO nanocomposites exhibited evidently stronger anti-*E. coli* activity, confirming the existence of synergistic effect between Ag and MgO. Moreover, this strong synergistic inhibition resulted in low Ag^+ release and toxicity of Ag–MgO nanocomposites [49]. Ciacotich et al. examined the antibacterial effect of electroplating copper-silver alloy coatings on stainless steel surfaces. SEM images showed that the prepared copper-silver coating had a significant pore structure and exposed area, increasing the chance of contact with bacteria. Moreover, the electroplated silver-copper surface has a higher roughness, further enhancing the contact bactericidal effect and the release of antimicrobial ions [50]. Garza-Cervantes et al. used a combination of silver with Zn, Co, Cd, Ni, and Cu to treat *E. coli* and *Bacillus subtilis* (*B. subtilis*), respectively. It was found that the antibacterial performance of the combination increased 8-fold compared to the treatment alone, suggesting that a synergistic effect occurred between the combined multi-metals. Moreover, at sub-inhibitory concentrations, silver/(Cu, Ni and Zn) increased the permeability of prokaryotic cells, speculating that this could be a mechanism for the synergistic behavior [51].

3.2. Photocatalytic composite type

Photocatalytic composite type refers to combining antibacterial components with photocatalytic propertity (i.e., ZnO, WO_3, ZrO_2) with other antibacterial metal active components. Thus, the composite materials could exhibit superior antibacterial activity in the condition either with light irradiation or not. Naz et al. used co-precipitation technique to dope copper and magnesium into ZnO-NPs. The UV–Visible absorption peaks of the metal-doped ZnO-NPs were increased and the energy band gap was red-shifted. Furthermore, the prepared doped ZnO-NPs showed a very high degradation rate of methyl blue, causing the color of methylene blue dye samples to almost disappear in 2–3 min, and a larger range of inhibition zones for *Klebsiella* and *Staphylococcus aureus* compared to pure ZnO-NPs formed. The authors concluded that with doped metal amount increase, more defect sites were created in the ZnO nanolattice. These defect sites inhibited the complexation of photogenerated electrons and holes, resulting in higher ROS levels and better antibacterial properties [52]. Hong et al. prepared Cu_2O–Ag/ZnO ternary nanocomposites by hydrothermal and chemical modification methods. Compared with single Cu_2O or Ag-modified ZnO, Cu_2O and Ag co-modified ZnO nanocomposites remarkably enhanced antibacterial activity. Moreover, Cu_2O and Ag nanoparticles were uniformly dispersed on the ZnO surface, avoiding the agglomeration of nanoparticles [53].

3.3. Rare earth activated type

Rare earth activated material is a compound of rare earth metals and antibacterial metals, enhancing the antibacterial activity of the material by the unique electron structure of rare earth metals. Rare earth elements doped with antibacterial components can create a synergistic effect and enhance the antibacterial capability of the material. As a result of the addition of the rare earth element Pr, Li et al. found that the inhibitory effect of Zn-doped amorphous silica on *E.coli* increased from 75.56% to 95.24% [54]. Similarly, Jiang et al. demonstrated, in their experiments, that the addition of rare earth elements can create a synergistic antibacterial effect [55]. In order to clarify the mechanism of the synergistic effect, the authors examined the loading and release of zinc ions and the production of ROS in the material before and after the addition of the rare earth element Lu. With the addition of Lu elements, the loading and release of zinc ions in the material as well as the production of ROS increased [55]. Yang et al. examined the specific surface area and pore size of the materials before and after the addition of Er elements [56]. This is because rare earth elements can decrease the surface energy of the material and avoid agglomeration of antibacterial components. As a result, there is an increase in the specific surface area, which enhances the contact area between the antibacterial material and bacteria. Moreover, the reduction of pore size enhances the adsorption performance of the material and increases the loading of the antibacterial active component, which improves the antibacterial effect of the material [53]. One the other hand, rare earth elements can extend the visible light absorption range of photocatalytic antibacterial active components as well as inhibit electron-hole compounding, leading to enhanced photocatalytic performance and more ROS production [57]. Using Ce doped into TiO_2, Gao et al. extended the photocatalytic effective wave length to visible light, resulting in a large amount of hydroxylic radical, even without ultraviolet light irradiation [58]. Ramya et al. discovered that in the Eu–Ag co-doped TiO_2 composites, the rare earth element Eu could capture some electrons for the reduction of Eu^{3+}, decreasing the electron-hole pair complexation rate. As a result, this increases the surface activity of TiO_2 and the efficiency of photocatalysis, as well as the antibacterial of Ag^+ [59]. In addition, rare earth elements are capable of filling the trap state of TiO_2 as electron donors, extending the lifetime of photogenerated electrons and generating more ROS, thus increasing the antibacterial effect [60].

4. Carriers

As another important component of antibacterial materials, the carries (also is called support) plays a significant role in supporting and dispersing the loaded active component. The physicochemical properties of carries significantly influence the distribution and state of active component and even will have a synergic interaction with the active component, which finally affect the antibacterial performance of antibacterial materials. Carriers generally have rich pore size structures and huge surface area, which can adsorb and slow-release active components in different ways. In addition, some carriers with special

biocompatibility can not only bind well with active components but also do not cause immune rejection by the human biological system, making it possible in clinical treatment. In this review, the carriers were classified into biocompatible and adsorptable types according to their functionalities, which were described below in detail along with their structural characteristics and antibacterial effects.

4.1. Biocompatible carriers

Biocompatible carriers (Fig. 8) [61,62] can prevent the body's immune system from treating them as foreign substances to trigger immune reactions after entering the organism. This type of carriers such as hydroxyapatite (HAP) and bioactive glasses (BG) are mainly used in dental materials, organ stents, drug carriers, and other clinical therapeutic applications.

4.1.1. Hydroxyapatite

Hydroxyapatite (HAP) is an important component of mammalian bones and teeth, accounting for approximately 70% by weight of human bone [63]. The similarities to calcified tissues in vertebrates provide it with excellent biocompatibility. Moreover, HAP has excellent osteoinductive and osteopathic properties [64], greatly broadening its application [65]. However, when used as an orthopedic implant, inhibiting the proliferation of microorganisms on its surface is a critical step in the therapeutic process.

It has been reported that pure HAP has few inhibitory effects on the growth of bacteria [66,67]. Nevertheless, HAP contains many trace cations (Zn^{2+}, Na^{+}, Mg^{2+}, etc.) and possesses a hexagonal crystal structure and these characteristics are favorable for the exchange with ions which possesses the similar charge type and ionic radius [68,69]. Consequently, HAP was often doped with antibacterial active components to enhance its antibacterial properties. Kumar et al. obtained strontium-doped hydroxyapatite (Sr-HAP) by wet chemical precipitation and compared the antibacterial effect with pure HAP against *E. coli* and *Sporosarcina pasteurii* (*S. pasteurii*). Sr-HAP inhibited both bacteria significantly after 2 h exposure [75]. In addition to the doping of Sr, Ag, Zn, Cu, Mg and Ce have also been successfully added to the HAP. The antibacterial effects of several HAPs doped with various ingredients are listed in Table 2. Besides, the crystallinity of HAP decreases with the increase of dopant ion concentration, but its thermal stability improves [74,76,77]. Priyadarshini et al. synthesized Ce-HAP samples with various Ce content by sol-gel method and evaluated their hemocompatibility, antibacterial activity, as well as biocompatibility. Diffuse reflectance spectroscopy (DRS) showed that with the addition increase of Ce^{4+}, the band gap value of HAP gradually decreased from 5.03 eV to 2.37 eV, accompanied with the decrease of the width & peak intensity of HAP crystal structure. As the replacement of Ca^{2+} by Ce^{4+}, the crystallinity and crystallite of the HAP structure were decreased, while the inhibition regions of *S. aureus*, *Bacillus subtilis*(*B. subtilis*), *E. coli,* and *P. aeruginosa* were broadened [74]. After several years' research, HAP doped with various antibacterial metals have been successfully synthesized and the study is no longer limited to general physicochemical properties but focuses on biological evaluation. Moreover, after doping with metal elements, the biocompatibility, degradability, osteoconductivity, and antibacterial properties of HAP could be effectively improved, providing a solid basis for the biomedical application of HAP in Biomedicine.

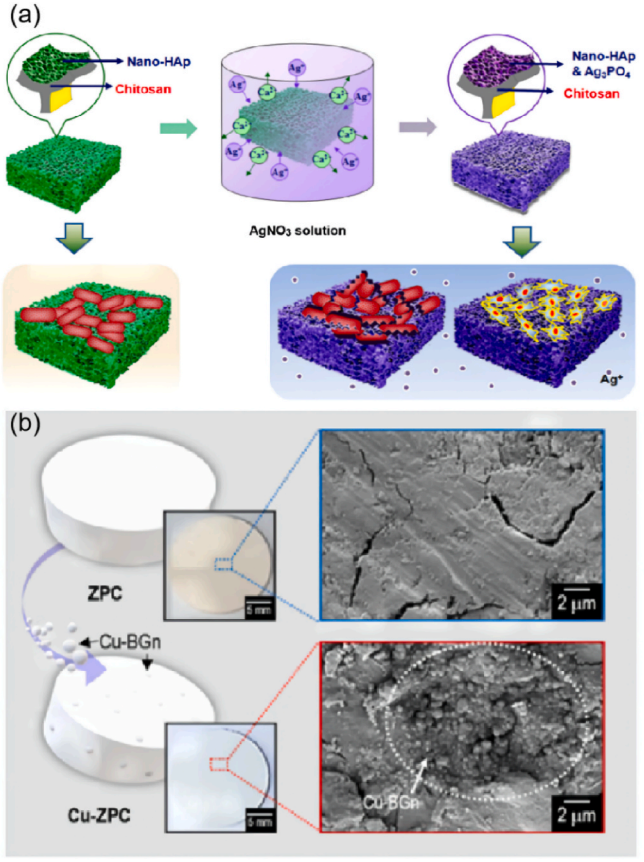

Fig. 8. Biocompatible carriers loaded with metal antibacterial active components (a) Silver loaded hydroxyapatite; (b) Copper loaded bioactive glass.

4.1.2. Bioactive glass

Bioactive glass (BG) is a type of glass biomaterials composed of oxides of silicon, sodium, calcium, and phosphorus. BG was firstly synthesized by Larry Hench [78]. After continuous improvement, the new generation of BG possesses excellent biocompatibility and mechanical stability. Moreover, as implants, they are biodegradable in the human body and can avoid foreign body rejection, making them highly valuable for clinical applications. As an important medical implant material, the prevention of pathogenic microbial infections and the avoidance of secondary surgery are guarantees of successful implantation. It has been shown that 80% of infections caused by microorganisms are related to biofilm formation [82]. Thus, enhancing the antibacterial effect of BG has become a current research hotspot. Munukka et al. revealed that BG have a certain antibacterial ability to inhibit the growth of pathogenic microorganisms such as *E. coli*, *S. aureus*, *P. aeruginosa*, and *Streptococcus mutans* (*S. mutans*) [83]. The pure BG relies on changing the surrounding pH and osmotic pressure to inhibit the growth of bacteria, yet the antibacterial effect is not very satisfactory [84]. To further improve their antibacterial ability, active components with antibacterial properties have been introduced to BG and BG with highly ordered channel structures have been well developed for better incorporating the extraneous antibacterial components. The antibacterial activity of the BG containing the metal component is presented in Table 3. Ryan et al. developed a multifunctional collagen BG scaffold loaded with copper ions (CuBG-CS) and added it to brain heart infusion (BHI) broth containing *S. aureus*. The CuBG scaffold containing 0.3 mg Cu^{2+}/ml was found to have significant antibacterial activity, inhibiting up to 66% of *S. aureus* and having no side effects on mammalian cells during the 28-day test period, reflecting the favorable biocompatibility of the BG for mammals [85]. Anand et al.also reported that zinc doping could effectively enhanced the mechanical strength of BG [86]. In a word, BG loaded with antibacterial components not only enhances the antibacterial effect but also provides favorable compatibility with living organisms, resulting in promising applications in the field of medical biomaterials.

4.2. Adsorptable carriers

Adsorptable carriers (Fig. 9) [87,88], i.e., zeolites, clay minerals,

Table 2
Antibacterial activity of HAP doped with common elements.

Doping elements	Preparation methods	Content	Microorganisms	Antibacterial effect	References
Ag	precipitation method	1.5 M	*S. aureus*	Z = 17 ± 0.51 mm	[70]
	Microwave method	1%	*E. coli*	MIC = 10.76 μg/mL	[71]
			P. aeruginosa	MIC = 5.38 μg/mL	
			S. aureus	MIC = 10.76 μg/mL	
		2%	*E. coli*	MIC = 6.12 μg/mL	[71]
			P. aeruginosa	MIC = 6.12 μg/mL	
			S. aureus	MIC = 6.12 μg/mL	
		3%	*E. coli*	MIC = 8.37 μg/mL	[71]
			P. aeruginosa	MIC = 2.09 μg/mL	
			S. aureus	MIC = 4.18 μg/mL	
		5%	*E. coli*	MIC = 11.50 μg/mL	[71]
			P. aeruginosa	MIC = 2.87 μg/mL	
			S. aureus	MIC = 5.75 μg/mL	
Zn	Wet chemical method	1.0 wt%	*E. coli*	Z = 20 mm	[72]
			S. aureus	Z = 7.0 mm	
		2.5 wt%	*E. coli*	Z = 22.7 mm	[72]
			S. aureus	Z = 8.0 mm	
Mg	Microwave method	Ca: Mg = 0.90:0.1(M)	*E. coli*	Z = 12.66 ± 1.15 mm	[73]
			P. aeruginosa	Z = 14.33 ± 0.57 mm	
			S. aureus	Z = 12.33 ± 0.57 mm	
			B. subtilis	Z = 13.33 ± 1.52 mm	
Ce	Sol-gel method	0.5%	*E. coli*	Z = 10 mm	[74]
			P. aeruginosa	Z = 4 mm	
			S. aureus	Z = 9 mm	
			B. subtilis	Z = 3 mm	
		0.75%	*E. coli*	Z = 13 mm	[74]
			P. aeruginosa	Z = 5 mm	
			S. aureus	Z = 10 mm	
			B. subtilis	Z = 4 mm	
		1%	*E. coli*	Z = 15 mm	[74]
			P. aeruginosa	Z = 7 mm	
			S. aureus	Z = 13 mm	
			B. subtilis	Z = 7 mm	
		1.25%	*E. coli*	Z = 18 mm	[74]
			P. aeruginosa	Z = 9 mm	
			S. aureus	Z = 15 mm	
			B. subtilis	Z = 8 mm	

[1]Z represents the diameter of the inhibition zone.

etc., have a well-developed pore structure and huge specific surface area, providing a good condition for the load and dispersing antibacterial active components, where the agglomeration of antibacterial active components with high surface energy could be avoided, thus enhancing the overall antibacterial effect. Common adsorption type carriers include.

4.2.1. Zeolites

As a typical support material, zeolite is three-dimensional crystalline hydrated aluminosilicate composed of [AlO_4] and [SiO_4] interconnected with oxygen atoms [89]. The continuous channels and relatively uniform pore size in the infinitely extended three-dimensional mesh structure inside zeolites provide a large specific surface area and a positive ion exchange capacity. Due to the substitution of Al^{3+} for Si^{4+} in zeolites, an electrovalence imbalance occurs within aluminum-oxygen and silicon-oxygen tetrahedra, making them susceptible to cation exchange [90]. Therefore zeolites are used to load metal antibacterial active components. Table 4 summarizes the effects of antibacterial materials with zeolites as carriers. In the literature, antibacterial properties may be enhanced when the antibacterial active component is loaded onto the support [91]. Inoue et al. found that hydroxyl radicals were generated in the solution illuminating the silver-loaded zeolite and measuring the ESR spectra. Moreover, *E. coli* lost the ability to form colonies after 5 min of exposure to silver-loaded zeolite under light, confirming the efficient antibacterial performance of it [92]. It is believed that zeolites enhance antibacterial activity by preventing the agglomeration of active components and increasing the effective area of contact with bacteria [93]. Hu et al. prepared silver-based 4A zeolite composites and showed that AgNPs were dispersed uniformly throughout the 4A zeolite, without aggregation [100]. Similarly, Abed et al. demonstrated that in the synthesized zeolite/silver-graphene oxide nanocomposites, silver particles were evenly dispersed in the zeolite [101]. On the other hand, the morphology of zeolite also has an effect on the antibacterial activity. Zeolites can have different levels of bacteria contact due to their shapes. Smaller sized zeolites, such as nano zeolites, have some advantages in ion exchange and ion release [102]. Chen et al. tested silver-loaded nanostructured zeolites (Ag-nZeo) and microsized zeolites (Ag-mZeo) for silver ion release and MRSA killing, and their results are shown in Fig. 10. While Ag-mZeo (400 μg/mL) completely killed MRSA within 7 min, Ag-nZeo (400 μg/mL) took 3 min. This indicates that the efficient killing rate of Ag-nZeo is closely related to its rapid silver ion release property [103]. Besides, Iyigundogdu et al. investigated the stability of zeolites containing silver and zinc ion exchange. Composites were found to have higher long-term antibacterial properties as the zeolite concentration increased [104]. Therefore, zeolites also play a role in the slow release of antibacterial active components.

4.2.2. Clay minerals

Clays are long-established traditional medicinal soil. As early as the Neanderthal period, people applied mud to the body in imitation of animals to clean the skin and treat wounds [105]. However, not all clays are bactericidal [106]. Moreover, clays can only exhibit antibacterial properties in the hydrated state (paste), where they are effective against

Table 3
Antibacterial effect of bioactive glass after doping with common elements.

Doping elements	Preparation methods	Content	Microorganisms	Antibacterial effect	References
Ag	Sol-gel method	0.05 g 0.16 mg/mL	*S. mutans*	Z = 12.83 ± 1.44 mm MIC = 2.5–5 mg/mL MBC = 5–10 mg/mL	[79]
	Solid-state reaction	1%	*Porphyromonas gingivalis* (*P. gingivalis*) *S. mutans* *Streptococcus sanguis* (*S. sanguinis*) *Enterococcus faecalis* (*E. faecalis*)	MIC = 1 mg/mL MIC = 8 mg/mL MIC = 8 mg/mL MIC = 16 mg/mL	[80]
		3%	*P. gingivalis* *S. mutans* *S. sanguinis* *E. faecalis*	MIC = 1 mg/mL MIC = 2 mg/mL MIC = 4 mg/mL MIC = 8 mg/mL	[80]
Mg	Sol-gel method	–	*E. coli* *P. aeruginosa* *S. aureus*	MIC = 15.62 mg/mL	[81]
	Solid-state reaction	1%	*P. gingivalis* *S. mutans* *S. sanguinis* *E. faecalis*	MIC = 4 mg/mL MIC = 2 mg/mL MIC = 8 mg/mL MIC>24 mg/mL	[80]
Sr	Solid-state reaction	1%	*P. gingivalis* *S. mutans* *S. sanguinis* *E. faecalis*	MIC = 2 mg/mL MIC = 2 mg/mL MIC = 8 mg/mL MIC>24 mg/mL	[80]
Zn	Solid-state reaction	1%	*P. gingivalis* *S. mutans* *S. sanguinis* *E. faecalis*	MIC = 4 mg/mL MIC = 2 mg/mL MIC = 8 mg/mL MIC = 2.5–5 mg/mL	[80]
Ga	Solid-state reaction	3%	*P. gingivalis* *S. mutans* *S. sanguinis* *E. faecalis*	MIC = 8 mg/mL MIC = 2 mg/mL MIC = 24 mg/mL MIC>24 mg/mL	[80]

specific bacteria [107]. In the literature [108–110], mineral metal ions dissolved within clays produce the main antibacterial effect, such as iron, copper, and zinc ions. Therefore, metal active components are added to clays used as support. Table 5 summarizes the effects of antibacterial materials with clay minerals as carriers. Clays are a convenient way to keep active components stable, as well as to avoid using stabilizing agents, thus reducing environmental hazards [111]. Moreover, they have a large specific surface area and a rich pore structure, thus providing many loading sites for active components. In addition, clays overcome the van der Waals gravitational force between nanoparticles to prevent agglomeration of the active components [112]. As mentioned above, the synergistic effect between clays and active components increases the.

antibacterial efficiency [120]. Shu et al. loaded ZnO onto halloysite nanotubes (HNTs) and investigated its inhibitory effect against *E. coli*. As a result, compared with the same dose of pure ZnO, the ZnO/HNT combination showed an even greater inhibitory effect on bacterial growth. This is because a homogeneous distribution of ZnO offers a larger effective contact area with bacteria. It also allows more active sites to produce ROS, thus increasing the antibacterial properties of the material [121]. To identify the adsorption efficiency of clays on antibacterial active components, Benli et al. measured the absorption of silver and zinc ions by sepiolite. The experimental data were found to be consistent with the Langouin isotherm model. Therefore, this indicates that silver and copper ions are forming a monolayer on the sepiolite surface. Another finding was that the absorption concentrations of silver and copper ions by sepiolite were 50 mg/g and 80 mg/g, respectively. With this, a theoretical basis is provided for the application of clays in antibacterial carriers.

5. Coating methods

The application of antibacterial materials has been achieved in two main ways: (1) antibacterial materials are added to the articles during the preparation process to obtain antibacterial effect, such as co-blending method; (2) the antibacterial material is sprayed on the surface of the article to form a protecting layer (film) to inhibit the multiplication of microorganisms to growth [122]. For method (1), despite of the simplicity of the direct blending method, it is difficult to distribute antibacterial active components uniformly in the matrix limited by the dispersibility and compatibility. In contrast, the spraying technique (method (2)) can form a uniform antibacterial film with a superior antibacterial effect. Commonly, the coating could be achieved via the methods like vapor deposition, electrodeposition, sputtering, sol-gel, arc spray, dip coating, spin coating, layer-by-layer, electrostatic spinning, etc. Table 6 summarizes the coating methods and characteristics of common metallic antibacterial materials. The antibacterial coatings formed on the surface of articles using the above methods achieve self-cleaning and antibacterial action on contact surfaces by two ways of releasing active components and resisting bacterial adhesion [123].

5.1. Active component release type coating

This type coating means releasing the antibacterial active components from the loaded coating, thus eliminating the surrounding adherent bacteria. The release of ions is an important factor affecting the antibacterial effect. After being released, antibacterial active components attack negatively charged bacteria, disrupting the cell wall (membrane). Eventually, the material inside the cell flows out and causes cell death. Moreover, they can induce oxidative stress in cells and cause cell death by producing large amounts of ROS and inhibiting the synthesis of proteins and nucleic acids. Oliverius et al. evaluated the ability of a new surgical dressing, StopBac, to combat post-operative abdominal infections, prepared by depositing a polymeric colloidal solution containing Ag^{+} on a pad via the spray method. This polymeric nano matrix can effectively control the release of Ag^{+} for a long time.

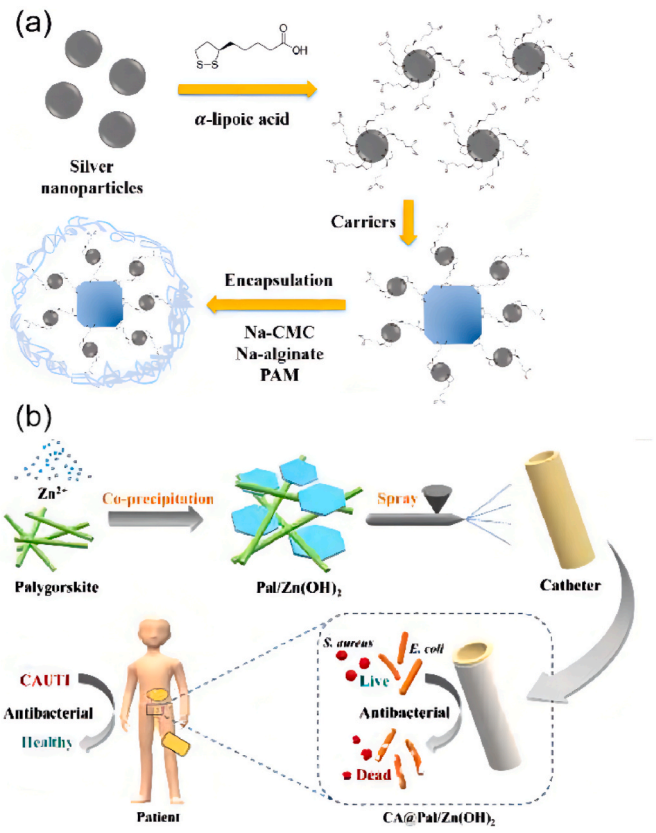

Fig. 9. Adsorptable carriers loaded with metal antibacterial active components (a) Silver loaded Linder type A zeolite; (b) Zinc loaded palygorskite clay minerals.

Among the patients tested, only one case developed a postoperative infection, demonstrating the effectiveness of this dressing in inhibiting the growth of microorganisms [124]. Guo et al. produced a silver-loaded composite coating by dipping the poly-L-lysine (PLL)/sodium alginate (SA)/PLL coating deposited with dopamine into $AgNO_3$ solution. Based on the results of the inhibition zone and the optical density measurements, the silver-loaded composite coating was found to be able to inhibit the proliferation of *S. aureus* and *S. mutans* completely within 24 and 48 h. Furthermore, Ag^+ can be released in this coating for more than 27 days, where the cumulative silver release in the first 6 days is approximately equal to the release in the last 21 days [125]. Similarly, Lia et al. immersed a wollastonite coating in a silver nitrate solution to load silver and measured the silver release rate by ICP-OES in deionized water. Surprisingly, the coating sustained the release of silver for up to 50 days [126].

5.2. Antibacterial adhesion type coating

The antibacterial activity of release-based coatings is restricted by the limited antibacterial activity of components, which will gradually decline with time. To ensure the stability and durability of the antibacterial effect, antibacterial coatings have been developed to prevent bacterial adhesion. The initial antibacterial adhesion coating does not kill microorganisms directly but is designed to prevent bacterial adhesion and non-specific protein uptake, curbing the formation of bacterial biofilms [127]. It was discovered that planktonic bacteria are more likely to adhere to hydrophobic surfaces, causing infections due to microorganisms attached to medical devices. Moreover, the microorganisms firmly attached to medical devices are very difficult to remove [128]. Thus, efforts must be made to develop a more effective coating to prevent bacterial adhesion. Among various coatings, antibacterial superhydrophobic coating was viewed as ideal to prevent bacterial adhesion [129]. The superhydrophobic coating inspired by the lotus leaf has a large contact angle and a small roll angle. The synergistic effect between its unique surface morphology and surface chemistry can significantly reduce its adhesion to bacteria, which can be removed from the adhered surface by a slight external force [130]. Although the superhydrophobic coating is a relatively green antibacterial method, research shows that its antibacterial properties will be greatly reduced or even disappear when the concentration of bacteria is too high [131]. Adding an antibacterial component to the superhydrophobic coating seems to be a good choice to address the problem above. The obtained antibacterial hydrophobic coating not only could prevent the attachment of bacteria by space repulsion and electrostatic repulsion but also was able to release antibacterial active components to destroy the structure of adhering bacteria, exhibiting antibacterial ability (Fig. 11) [132]. Li et al. successfully loaded AgNPs on the superhydrophobic stainless steel meshes by combining both double potential deposition and in situ polymerization grafting method. The water contact angles increased from 99.9° to 160.6° after modifying the deposited surface.

Table 4
Antibacterial effect of zeolites after doping with common metals.

Species of zeolites	Doping elements	Microorganisms	Antibacterial effect	References
NaY zeolite				
Ag(1)-Y	Ag	*E. coli*	MIC = 0.4 g/L	[94]
		S. aureus	MIC = 4 g/L	
ZS25	Ag	*E. coli*	Z = 1.83 ± 0.04 mm	[95]
		S. aureus	Z = 1.83 ± 0.04 mm	
ZS50	Ag	*E. coli*	Z = 2.08 ± 0.04 mm	[95]
		S. aureus	Z = 1.85 ± 0.00 mm	
ZS100	Ag	*E. coli*	Z = 2.58 ± 0.04 mm	[95]
		S. aureus	Z = 1.83 ± 0.04 mm	
ZS25	Ag	*E. coli*	Z = 2.93 ± 0.04 mm	[95]
		S. aureus	Z = 1.85 ± 0.00 mm	
13X zeolite				
X–ZnO	ZnO	*E. coli*	MIC = 0.12–0.24 mg/mL	[96]
ZnO-13X	ZnO	*E. coli*	MIC = 1.0 mg/mL MBC = 4.0 mg/mL	[97]
		S. aureus	MIC = 0.8 mg/mL MBC = 4.0 mg/mL	
Cu^{2+}/ZnO-13X	ZnO Cu	*E. coli*	MIC = 0.2 mg/mL MBC = 0.8 mg/mL	[97]
		S. aureus	MIC = 0.4 mg/mL MBC = 1.0 mg/mL	
zeolite 4A				
Cu-zeolite 4A	Cu	*E. coli*	MIC = 625 μg/L	[98]
		S. aureus	MIC = 1250 μg/L	
CuO/4A	CuO	*E. coli*	MIC = 3.0 mg/mL MBC = 4.0 mg/mL	[99]
		S. aureus	MIC = 5.0 mg/mL MBC = 5.0 mg/mL	
ZnO/4A	ZnO	*E. coli*	MIC = 2.0 mg/mL MBC = 3.0 mg/mL	[99]
		S. aureus	MIC = 4.0 mg/mL MBC = 5.0 mg/mL	

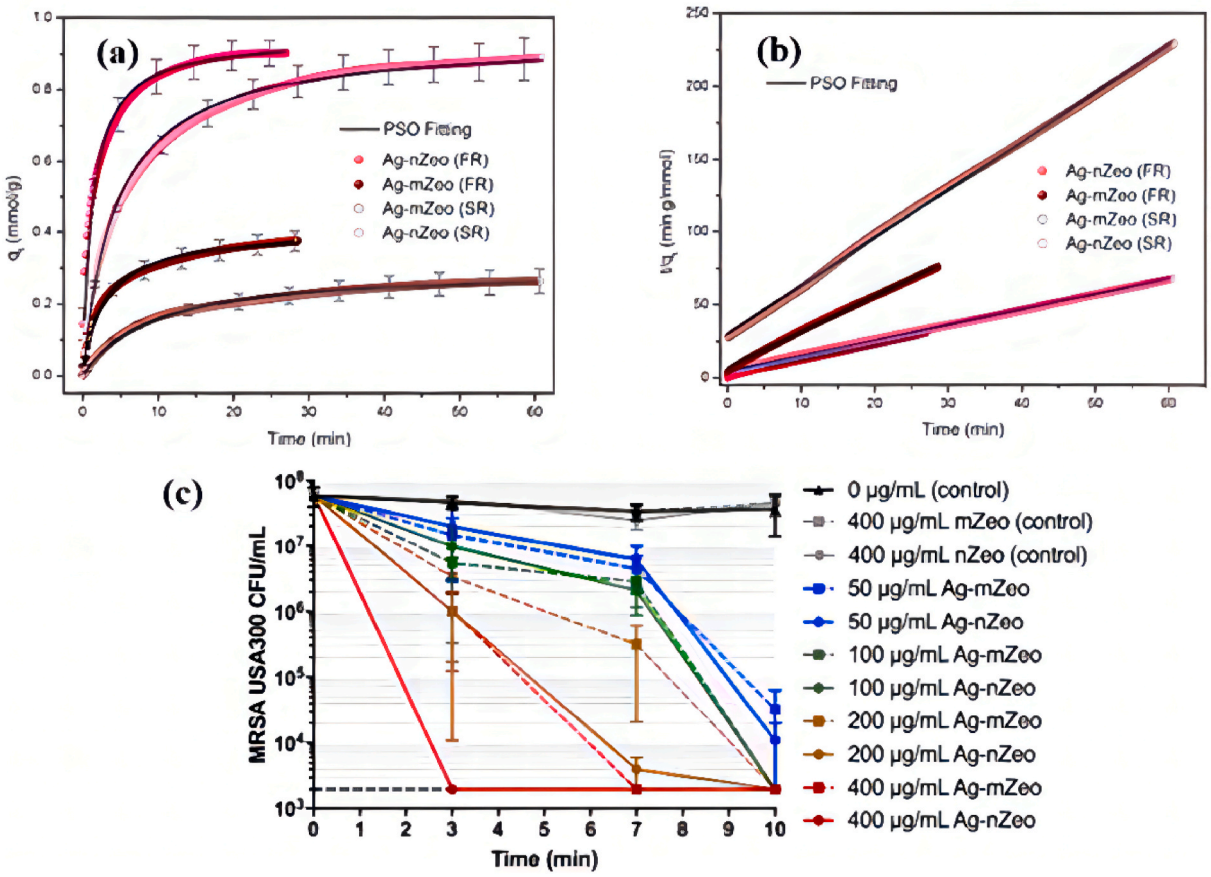

Fig. 10. Silver ion release and MRSA killing test results: (a) Average silver ion release kinetics curves of Ag-zeolites at fast rate (FR, 5.5 mL/min) and slow rate (SR, 0.6 mL/min). Error bars are shown in every 3 min; (b) Pseudo-second order (PSO) linear regression of silver release kinetics data; (c) Assessment of rapid killing ability of Ag-nZeo and Ag-mZeo.

Moreover, when the growth time of PDA@ODA(polydopamine @ octadecylamine)was 3600 s, the water droplets could roll off rapidly at an inclination angle of 5°, allowing the bacteria to be removed before forming a thick biofilm. As the electrodeposition time increased, the generated AgNPs become dense and form clusters, leading to a synergistic antibacterial effect with the superhydrophobic structure, which enhances its antibacterial ability [138].

6. Applications

The global climate change cause by the greenhouse effect provides suitable conditions for bacteria to multiply, which seriously threatens human health. Metal-based antibacterial materials are popular and widely used in all aspects of life because of their wide application range, strong bactericidal properties, and lack of antibacterial resistance [122]. Due to the occurrence of several cases of food packages with the new coronavirus, resulting increased attention to food safety. Here, the application of metal-based antibacterial materials for food storage under ambient and low temperatures will be mainly clarified.

6.1. Ambient temperature food packaging

Applying materials with antibacterial properties to food packaging films not only improves food safety to prevent food from being contaminated during processing and transportation but also extends its shelf life, reducing food waste with obvious economic and environmental benefits. Currently, most food packaging materials are based on plastic. Plastic films are widely used due to their low cost, processability, and high transparency [154]. However, with the increasing demand for freshness and safety of food products, traditional food preservation films are difficult to meet people's needs due to their poor antibacterial properties. Consequently, many scholars have modified these films to enhance the scope of application and properties. Rangaraj et al. added date syrup waste extract (DSWE) as an antioxidant to silver doped sepiolite hybrid (Ag-Sep) to prepare a series of gelatin/DSWE/Ag-Sep active composites. As shown in Fig. 12, the prepared composite was applied to apple slices to study its antibacterial and antioxidant properties. Compared to apple slices without film covering, the slices covered with this film remained exceptionally fresh after 5 h [155]. Similarly, the silver-loaded cellulose film prepared by Gu et al. allowed cherry tomatoes to remain fresh after 9 days of storage at 25 °C [156]. Kusalya et al. discovered that lemons and strawberries could be stored at room temperature for 10 days when wrapped in polyvinyl alcohol fiber films containing silver [157]. As well as inhibiting the proliferation of bacteria, the metal antibacterial active components reduced water vapor transmission in cling film additionally, extending the shelf life of fruits and vegetables. A study found that tomatoes and cabbage in bags sprayed with 10% AgNPs colloidal suspension did not lose moisture much after 7 days. In contrast, the vegetables in bags not sprayed with AgNPs colloidal suspension showed significant moisture loss [158]. Furthermore, Deng et al. revealed that grapes packed in polyvinyl alcohol composite film containing silver lost 8.37% of their weight after 10 days, significantly less than the 16.47% and 11.20% mass losses of unpacked and PVA groups, respectively. As AgNPs are evenly dispersed in the film, they hinder the transfer of water molecules in and out of the film [159]. Moreover, metal antibacterial active components can also improve the mechanical properties of the film, reducing the damage to the film during transportation. Jamroz et al. discovered that the

Table 5
Antibacterial effect of clay minerals after doping with common elements.

Species of clay minerals	Doping elements	Microorganisms	Antibacterial effect	References
Montmorillonite				
B-550T/Ag	Ag	*E. coli*	Z = 13.3 mm MIC = 2.5 mg	[113]
B–300S/Ag	Ag	*E. coli*	Z = 12.3 mm MIC = 1.0 mg	[113]
Zn/MMT	Zn	*E. coli*	MIC = 8.0 mg/mL	[114]
		S. aureus	MIC = 4.0 mg/mL	
Ce/MMT	Ce	*E. coli*	MIC = 10.0 mg/mL	[114]
		S. aureus	MIC = 4.0 mg/mL	
Zn–Ce/MMT	Zn Ce	*E. coli*	MIC = 1.5 mg/mL	[114]
		S. aureus	MIC = 1.0 mg/mL	
Cu-MMT	Cu	*Aeromonas hydrophila*	MIC = 0.15 mg/mL MBC = 0.6 mg/mL	[115]
Kaolinite				
Ag-Kaol	Ag	*E. coli*	MIC = 8 mg/mL	[106]
		P. aeruginosa	MIC = 5 mg/mL	
		S. aureus	MIC>10 mg/mL	
CA-Ag-Kaol	Ag	*E. coli*	MIC = 12 mg/mL	[106]
		P. aeruginosa	MIC = 10 mg/mL	
		S. aureus	MIC = 5 mg/mL	
Zn-Kao-t1	Zn	*Stenetrophomonas maltophilia* (*S. maltophilia*)	MIC = 3 mg/mL	[116]
		Bacillus cereus	MIC = 9 mg/mL	
		E. coli	MIC>12 mg/mL	
C–Zn-Kao-t1	Zn	*S. maltophilia*	MIC = 3 mg/mL	[116]
		B cereus	MIC = 1 mg/mL	
		E. coli	MIC>12 mg/mL	
CuKaoF	Cu	*P. aeruginosa*	MIC = 8 mg/mL	[117]
CuKaolinite	Cu	*E. faecalis*	Z = 14.16 mm	[118]
Seafoam				
AgSep	Ag	*E. coli*	MIC = 50 mg/L Z = 5 mm	[119]
		S. aureus	MIC = 50 mg/L Z = 6 mm	[119]
CuSep	Cu	*E. coli*	MIC = 100 mg/L Z = 3 mm	[119]
		S. aureus	MIC = 100 mg/L	[119]

modulus of elasticity and elongation at break of the films increased with increasing concentration of Se-AgNPs [160]. Shankar et al. also reported an increase in tensile strength of agar/lignin composite films from 44.1 ± 3.6 MPa to 49.7 ± 3.3 Mpa after the addition of AgNPs [161]. The increased mechanical properties are likely a result of molecular forces between the components in the films, such as between hydroxyl groups in the biopolymers and AgNPs [162,163].

6.2. Low temperature food packaging

Public safety incidents caused by pathogenic bacteria carried through the cold chain food have occurred several times in recent years. Especially, more frequent since the outbreak of COVID-19, nearly 265 batches of frozen products were detected with novel coronavirus in 2021 alone, making the disinfection of cold chain items a major concern [164]. The improvement of food packaging technology under low temperatures is urgent to stop the spread of germs. Zare et al. prepared composites containing ZnO and silver nanomaterials by solvent casting method and directly packaged them against chicken breast at 4 °C to test the antibacterial effect of the nanocomposites at a low temperature state. With the increasing content of added nanomaterials, the survival rate of both *S. aureus* and *E. coli* decreased as shown in Fig. 13. The composite containing 3 wt% ZnO–AgNCs was relatively effective in antibacterial effect, which could reduce *E. coli* by more than 4 log in 4 h [165]. This provided a strong basis for the storage of meat products at low temperatures. Kuuliala et al. packaged fresh pork sirloin in LDPE films with silver that could be stored at 6 °C for 28 days [166]. In the literature, silver and bamboo containing nonwoven fabrics extend the shelf life of salmon fillets by 5 days as compared to cotton wrappers [167]. Similarly, Shao et al. discovered that raw shrimp stored at 4 °C with nanocomposite membranes containing ZnO retained good sensory properties for 12 days [99].

Metal-based antibacterial materials can not only extend the storage time of poultry and aquatic products but also show some advantages in the storage of fruits and vegetables. Despite the benefits of freezing, frozen fruits and vegetables still have shortcomings, such as the incapacity to inhibit the bacteria that grow at low temperatures. Under low-temperature conditions, however, it is possible to remedy this problem with antibacterial.

components added to cling film. Mousavi et al. [168] packaged fresh dates with composite films containing AgNPs (3% and 5% by weight) to test the storage effect at 0 °C and 4 °C. The dates packed with 5% AgNPs still present favorable sensory quality and lower acidity and reducing sugar than the control group (packed with Penguin freezer bags) after 53 days of storage at 4 °C, proving that the AgNPs material could effectively extend the storage time of fruits and vegetables at low temperatures. It has been shown that AgNPs can improve the storage time of fruits and vegetables by promoting the oxidation of ethylene and inhibiting the growth of microorganisms [169]. Moreover, the film containing AgNPs can reduce water loss and oxygen penetration in fruits and vegetables.

7. Toxicology

Currently, food safety is getting more and more attention. The use of metal-based antibacterial materials in food packaging can inhibit pathogenic microorganism growth, improve food sensory properties, and extend shelf life. Compared with food preservation technologies such as freezing and ray sterilization, the antibacterial packaging has the characteristics of low cost and excellent effect, which can fundamentally solve the attack of microorganism on food. Therefore, metal-based antibacterial materials play an important role in the field of food packaging and have become the focus of attention of researchers. Despite many advantages of metal-based antibacterial materials in food packaging applications, there are concerns about their toxicity. Studies have shown that metal-based nanoparticles (e.g., ZnO-NPs, AgNPs, etc.) entering the humans can cause different degrees of damage to the body and cells, induce allergies, cardiovascular diseases, and even genotoxicity to the human body [170–172]. Contacting with antibacterial food packaging can expose the body to nanoparticles or metal ions, which can pose health risks. Therefore, it is necessary to evaluate the migration of antibacterial components in food packaging. When orange juice was stored at 4 °C using LDPE film containing ZnO-NPs, Emamifar et al. discovered that after 112 days, the orange juice retained zinc ions in the level of (0.68 ± 0.002) μg/L [173]. Echegoyen et al. discovered that the

Table 6
Coating methods and characteristics of common metal-based antibacterial materials.

Methods	Features	Antibacterial active component	Process parameters	Substrate	Size	References
Chemical vapor deposition	With a columnar crystal structure.	Cu	Stirring speed:120 rpm; Flow rate to burner head:0.6 $lmin^{-1}$Heating temperature:75°C ± 3°C	Borosilicate glass	Films:25 nm	[133]
	Not resistant to bending. High coating purity and adhesion.	$CuCu_2O$	Heating temperature:350°C	Glass	copper films:200–300 nm; copper oxide films:0.4–1 μm	[134]
	Low cost. Strong deposition rate.	CuNPs	Curing temperature:390 °CDeposition temperature:350°C	Polydimethylsiloxane (PDMS)	CuNPs:3.56 ± 0.8 nm	[135]
		Cu Ag Zn	Flow Rate:100 μl/min; Electrical power: 60–500 W	Wood polymer composites(WPC)	–	[136]
Electrodeposition method	Simple process.	Cu	Current Density:20 mA cm^{-2}; Electrode:Rolled copper foils (99.9% copper)	Copper foils	Cu:1–5 μm	[137]
	Low cost.	AgNps	Voltage:−0.7 V、−0.1 VElectrodes:platinum plate、saturated calomel electrodeTemperature: 75 °C;	The superhydrophobic stainless-steel	AgNps:12–30 nm	[138]
	High efficiency.Precise regulation of film growth.	Cu_2O–ZnO	Current Density:5.0 mA/cm^2; Electrode:copper sheet (4 cm × 4 cm)、nickel foam (4 cm × 4 cm)	Nickel foam	Cu_2O–ZnO:851.8 nm-1.64 μm	[139]
Sputtering method	Uniform coating.	AgNps	Radio Frequency Power:200 W; Direct current power:1 W; The distance between targets and substrates:14 cm; Time:80 min; Pressure:5.5 dPa	Glass-fibre air filters Stainless-steel fibre-based air filters Cotton	Coating:300 nm	[140]
	Fast particle deposition speed.	Ag_3W	Radio Frequency Power:200 W; Direct current power:3 or 5 W	FFP3 masks	Coating:<200 nm	[141]
	Low utilization of target material.	CuNps	Pressure:Argon gas 8 × 10^{-4} Pa; Substrate moving speed:90 rpm; Time:60 min; Power:50 W	Bacterial cellulose	–	[142]
		ZnO-Nps	Pressure:1 Pa; Argon and oxygen flow:55 sccm and 5 sccm; Time:30 min; Power:100 W	BC/Cu	–	[142]
Sol-gel method	Low cost. Good film formation uniformity and stability. Simple operation	Cu Ag Zn	Traction speed:100 mm/min Pharmaceutical content:0.25 ma.% for silver and 1.5 ma.% for copper and zinc nitrate	WPC	–	[136]
Sol-gel method	Low cost.	Au ZnO	Stirring time:3 h; Aging time:24 h; Extraction speed:250 mm/s; Drying temperature:120°C Drying time:10 min; Calcination temperature:400°C; Calcination time:3 h	–	Films:24.91–39.22 nm	[143]
	Good film formation uniformity and stability.	TiO_2 Mn	Stirring temperature: 50°C Stirring time:1.0 h Evaporation temperature: Room temperature Evaporation time:48 h Calcination temperature:400°C Calcination time:1 h	Wall paint	Mn–N–TiO_2:2.075 μm	[144]
	Simple operation.	ZnO QDs	Stirring temperature:78°C Stirring time:30 min Centrifugal speed:3500 rpm Centrifugal time:5 min	–	ZnO quantum dots(ZnO QDs):3–6 nm	[145]
Wire arc spraying	High bonding strength between coating and substrate.High deposition efficiency.Simple equipment.	Cu	Feeding speed: 82 g/min; Spraying distance:100 mm; Current:200 A; Voltage:33 V	stainless steel 316	Coating:500 μm	[146]
	Thin and dense coating. Economical and energy-saving.	Ti(Zn)O_2 ZnO	The distance between targets and substrates:160 mm; DC arc current:70 A; Deposition time:27 min	Pure Ti substrates	Coatings:1.5 μm–1.8 μm	[147]

(*continued on next page*)

Table 6 (*continued*)

Methods	Features	Antibacterial active component	Process parameters	Substrate	Size	References
Dipping method	High efficiency.Suitable for mechanized production.	AgNPs	Dipping the dopamine-modified PSP coating into $AgNO_3$ solution	Titanium surface	AgNPs:20–30 nm.	[125]
	Limited by the shape of the item.	Graphene quantum dots (GQDs)	Immersion time:2 min、30 s; Drying temperature:80°C Drying time:5 min GQD introduction amounts:0.05、0.1、0.3 and 0.5 wt%	Polyamide film	GQDs:3.4–8.8 nm	[148]
Electrostatic spinning technology	Ease of operation.	TiO_2	Inner diameter of spinneret device:0.8 mm; Plastic nozzle inner diameter:2.0 mm; Voltage:22–24 kV; Flow Rate:2.0 mL/h; Distance between collector and tip:14–15 cm	Polyurethane nanofiber membrane	Polyurethane/TiO_2: 1258 nm	[149]
	Low efficiency.Low coating strength.	CuZn	Plastic Syringe:10 ml Feeding rate:3 μL/min; Electric field:1.16 kV/cm; Rotational Speed:100 rpm	Nanofibers(NF)	CuZn NFs: 19.2–299.4 nm	[150]
Surface immobilization	Formation of strong interactions between the antibacterial molecules and the membrane surface. Migration of active components is significantly limited.	AgNPs	Ultrasonic stirring temperature:25°C Ultrasonic stirring time:3 s; Rotary vibrating screen rate:20 rpm Mixing time of rotary shaker:24 h.	Polyamide film	AgNPs:30 nm	[151]
Layer by layer method	Technical simplicity.Low cost.	AgNPs	Substrate: LDPE film with a thickness of 0.04 mm Ultrasonic processing time:10 min; Ultraviolet wavelength:180–254 nm UV/ozone treatment time:30 min; Drying temperature:60°C Drying time:24 h Immersion time:15 min	LDPE	AgNPs:19–160 nm	[152]
	Applicability to almost any type of substrate.Possibility to control the physicochemical properties of the film surface.	AgNPs	Water bath temperature:95°C Curing time:2 min	Polyamide laminated film	AgNPs:20 nm	[153]

migration of AgNPs is primarily caused by nanoparticles being released from the package's surface and the oxidative dissolution of silver. During the migration process, most of the nanoparticles on the surface are released, while the remaining AgNPs are gradually oxidized to silver ions with time changes [174]. In order to clarify the migration of metal antibacterial components in food, researchers have discussed factors such as the acidity of the food, the temperature and pressure of environment, as shown in Fig. 14 [175–177]. It is widely accepted that the migration of nanoparticles increases in acidic conditions. This is because the high oxidation potential of an acidic environment reduces the electrostatic repulsion between nanoparticles, which leads to their aggregation and facilitates migration of more nanoparticles [178,179]. The migration of nanoparticles is also influenced by temperature. Liu et al. found that the release rate of ions from the synthesized AgNPs increased with increasing temperature in the range of 0–37 °C [180]. Additionally, Liu et al. examined the migration of copper in LDPE films containing CuNPs at different temperatures in 3% (w/v) acetic acid solution. They found that the maximum migration of copper at 70 °C was much higher than that at 40 °C [181]. The ease of material diffusion at high temperatures is probably a factor in the rise in nanoparticle mobility. It has been demonstrated that pressure has the potential to influence the migration of metal nanoparticles in addition to pH and temperature. Chi et al. observed that high pressure treatment at 200 to 400 MPa significantly inhibited the migration of AgNPs from PLA films [182]. In addition, Zhu et al. demonstrated that, in comparison to 300 and 400 MPa pressures, PLA composite films treated at 200 MPa migrated the least amount of AgNPs [176]. Despite the fact that numerous academics have examined the migration of metal antimicrobial agents in food packaging, no consensus has been reached. There is currently no established toxicity evaluation system for metal antibacterial components used in food packaging, and the research of the migration process and migration mechanism is still vague. To offer a solid foundation for their wider and safer application in the food industry, it is necessary to do more extensive research on the harmful effects of metal antibacterial components on human health and the migration in food.

8. Remarks and prospects

The misuse of antibiotics in recent years has made pathogenic microorganisms possess resistance. Nevertheless, metal-based antibacterial materials have unique low bacterial resistance, making them an attractive material for solving this issue. In this paper, the mechanism of metal-based antibacterial materials is analyzed, and classified into four categories: contact antibacterial, dissolution antibacterial, oxidative antibacterial, and substitution antibacterial. In the process of inhibiting pathogenic microorganisms, these four mechanisms interact and intersect. Moreover, based on the results of the studies conducted so far, it is hard to distinguish between them. Therefore, further experimental exploration by researchers is needed. As the most commonly used

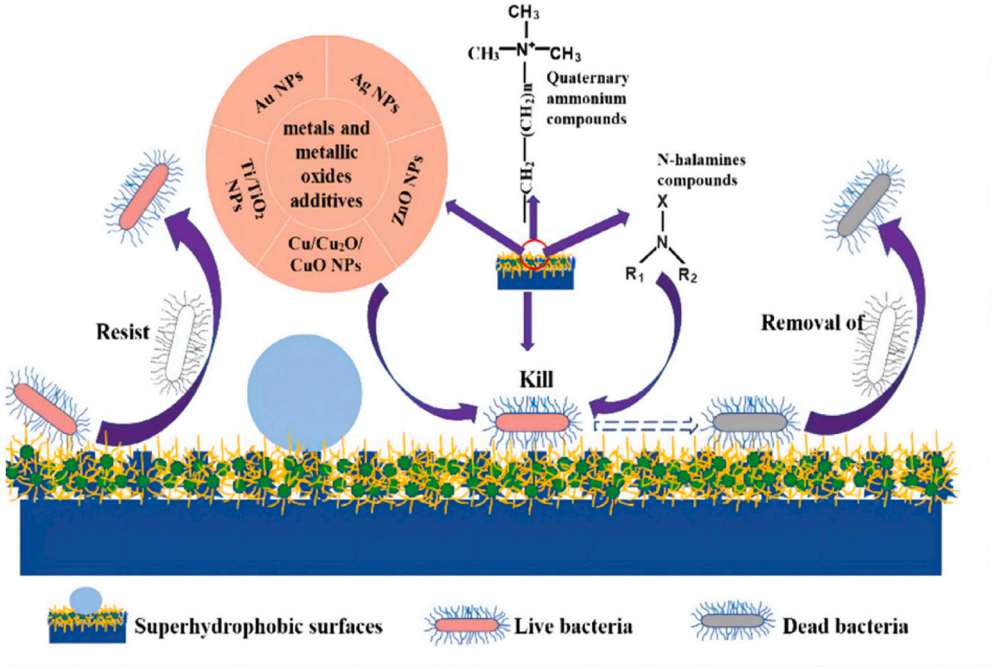

Fig. 11. The mechanism of action for antibacterial superhydrophobic coating.

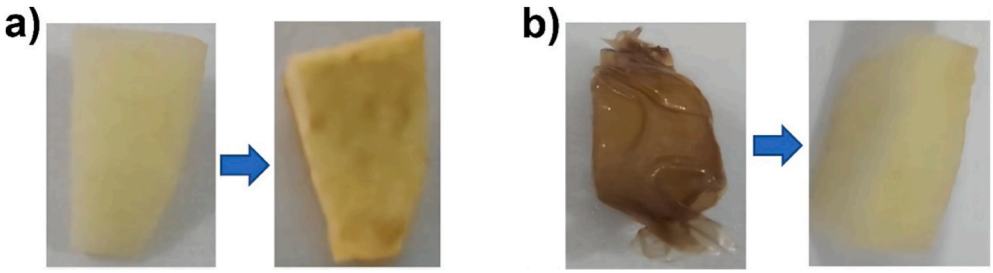

Fig. 12. Food preservation test: a) open control apple piece and b) apple sample covered with the GD-AS-2 composite film.

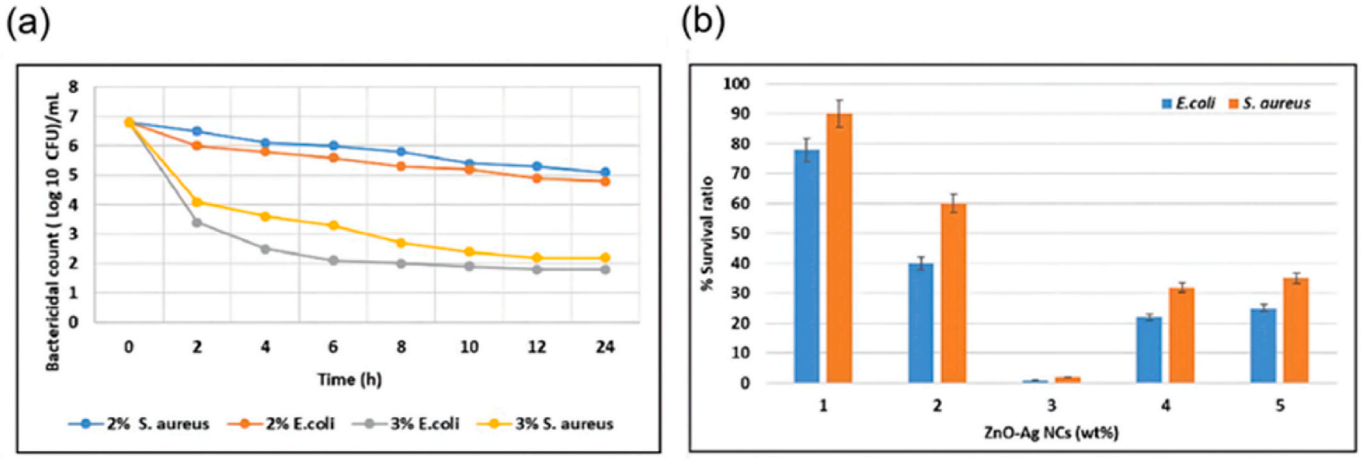

Fig. 13. ZnO–Ag antibacterial results: (a) Kinetics of the antibacterial activity NCs BP with 3.0 and 2.0 wt % loading against *E. coli* and *S. aureus*; (b) Effect of NCs BP on the survival ratio of *E. coli* and *S.aureus*. (zinc oxide: ZnO, silver: Ag, nanocomposites: NCs, biopolymer: BP).

antibacterial metals, silver, copper, and zinc have been applied in many fields. However, the single metal has irreparable defects. To improve this problem, the synergistic effect of multi-metal antibacterial components has proven to be an effective way. Multi-metal synergy is divided into three main points in this paper: metal composite, photocatalytic composite and rare earth activated, and the effect of synergy on antibacterial activity is discussed. Additionally, different types of carriers can give antibacterial materials special properties and broaden the range

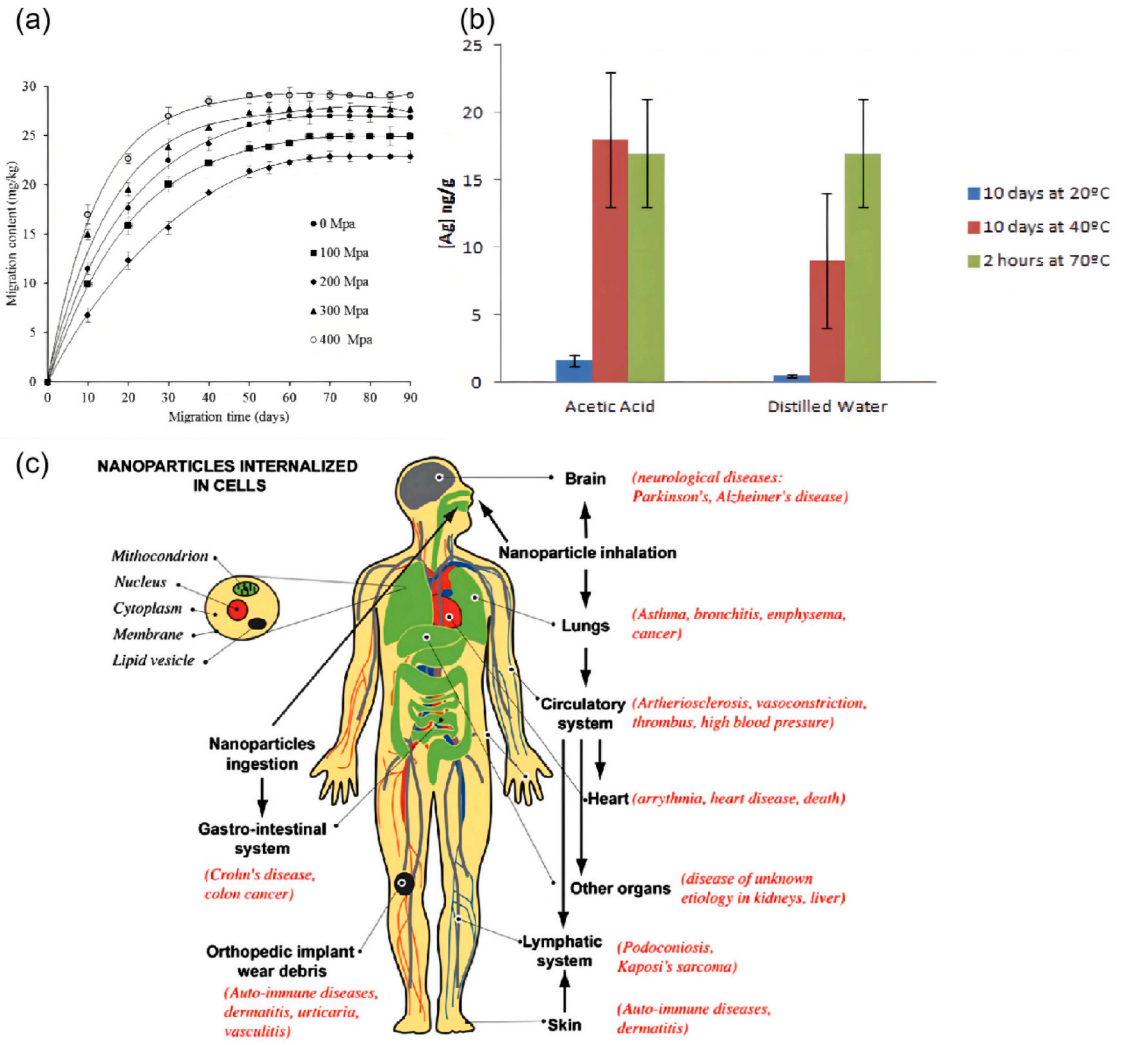

Fig. 14. Toxicity of nanoparticles and factors affecting their migration (a) Effect of pressure on migration of nanoparticles; (b) Effects of pH and temperature on the migration of nanoparticles; (c) Toxicity of nanoparticles to humans.

of applications in various fields. We focused on the analysis of adsorptable carriers and biocompatible carriers. As for the application of metal-based antibacterial materials, this paper highlights their application in food packaging because cold-chain food frequently carries pathogens. Nevertheless, there will be some damage to the human body as a result of metal ion release migration. Therefore, in order to facilitate metal antibacterial material development, an adequate evaluation system is needed. Moreover, how to balance the safety, efficiency, and stability of antibacterial materials will be an important research direction for future antibacterial materials.

CRediT authorship contribution statement

Xiaotong Yang: Conceptualization, Writing - Original Draft. **Qingjun Yu:** Conceptualization, Writing - Review & Editing. **Wei Gao:** Documents collection, assist writing. **Xiaoning Tang:** Review & Revise. **Honghong Yi:** Review & Revise. **Xiaolong Tang:** Supervision.

Declaration of competing interest

The authors declare that they have no known competing financial interests or personal relationships that could have appeared to influence the work reported in this paper.

Acknowledgments

This work was supported by the Open Research Fund Program of State Environmental Protection Key Laboratory of Food Chain Pollution Control (No. FC2021YB05), Fundamental Research Funds for the Central Universities (No. FRF-IDRY-20-004) and National Natural Science Foundation of China (No. U20A20130).

References

[1] W. LlU, Development of antimicrobial fiber and application of antimicrobial textiles, Chem. Fibers.Textil. Technol. 40 (2011) 22–27.
[2] X. Zhou, L. Huang, W. Zeng, J. Li, J. Huang, Sustained release performance and antibacterial properties of silver-doped calcium phosphate, J. Ceram. 42 (2021) 626–631.
[3] C. Murray, K. Ikuta, F. Sharara, C. Moore, Global burden of bacterial antimicrobial resistance in 2019: a systematic analysis, Lancet 399 (2022) 629–655.
[4] V. Nandakumar, C.N. Huang, A. Pulgar, V. Balasubramanian, G.H. Wu, P. Chandar, B.M. Moudgil, Particle assisted removal of microbes from surfaces, J. Colloid Interface Sci. 533 (2019) 190–197.
[5] P.K. Stoimenov, R.L. Klinger, G.L. Marchin, K.J. Klabunde, Metal oxide nanoparticles as bactericidal agents, Langmuir 18 (2002) 6679–6686.
[6] X.Q. Xing, W.S. Ma, X.Y. Zhao, J.Y. Wang, L. Yao, X.Y. Jiang, Z.H. Wu, Interaction between surface charge-modified gold nanoparticles and phospholipid membranes, Langmuir 34 (2018) 12583–12589.
[7] I. Sondi, B. Salopek-Sondi, Silver nanoparticles as antimicrobial agent: a case study on E-coli as a model for Gram-negative bacteria, J. Colloid Interface Sci. 275 (2004) 177–182.

[8] P. Liu, W.L. Duan, Q.S.I. Wang, X. Li, The damage of outer membrane of Escherichia coli in the presence of TiO_2 combined with UV light, Colloids Surf., B 78 (2010) 171–176.
[9] H. Wang, Y.J. Jiang, Y.S. Zhang, Z.W. Zhang, X.Y. Yang, M.A. Ali, E.M. Fox, K. S. Gobius, C.X. Man, Silver nanoparticles: a novel antibacterial agent for control of Cronobacter sakazakii, J. Dairy Sci. 101 (2018) 10775–10791.
[10] L.M. Gilbertson, E.M. Albalghiti, Z.S. Fishman, F. Perreault, C. Corredor, J. D. Posner, M. Elimelech, L.D. Pfefferle, J.B. Zimmerman, Shape-dependent surface reactivity and antimicrobial activity of nano-cupric oxide, Environ. Sci. Technol. 50 (2016) 3975–3984.
[11] N. Padmavathy, R. Vijayaraghavan, Enhanced bioactivity of ZnO nanoparticles-an antimicrobial study, Sci. Technol. Adv. Mater. 9 (2008), 035004.
[12] M.A. Ansari, H.M. Khan, A.A. Khan, S.S. Cameotra, Q. Saquib, J. Musarrat, Interaction of Al_2O_3 nanoparticles with Escherichia coli and their cell envelope biomolecules, J. Appl. Microbiol. 116 (2014) 772–783.
[13] F. Mirzajani, A. Ghassempour, A. Aliahmadi, M.A. Esmaeili, Antibacterial effect of silver nanoparticles on Staphylococcus aureus, Res. Microbiol. 162 (2011) 542–549.
[14] Z.M. Xiu, Q.B. Zhang, H.L. Puppala, V.L. Colvin, P.J.J. Alvarez, Negligible particle-specific antibacterial activity of silver nanoparticles, Nano Lett. 12 (2012) 4271–4275.
[15] Q.L. Feng, J. Wu, G.Q. Chen, F.Z. Cui, T.N. Kim, J.O. Kim, A mechanistic study of the antibacterial effect of silver ions on Escherichia coli and Staphylococcus aureus, J. Biomed. Mater. Res. 52 (2000) 662–668.
[16] W.R. Li, X.B. Xie, Q.S. Shi, S.S. Duan, Y.S. Ouyang, Y.B. Chen, Antibacterial effect of silver nanoparticles on Staphylococcus aureus, Biometals 24 (2011) 135–141.
[17] L. Macomber, J.A. Imlay, The iron-sulfur clusters of dehydratases are primary intracellular targets of copper toxicity, Proc. Natl. Acad. Sci. U. S. A 106 (2009) 8344–8349.
[18] S.J. Kang, Y. Il Cho, K.H. Kim, E.S. Cho, Proteomic analysis to elucidate the antibacterial action of silver ions against bovine mastitis pathogens, Biol. Trace Elem. Res. 171 (2016) 101–106.
[19] W.S. Abbas, Z.W. Atwan, Z.R. Abdulhussein, M.A. Mahdi, Preparation of silver nanoparticles as antibacterial agents through DNA damage, Mater. Technol. 34 (2019) 867–879.
[20] R. Singh, S. Cheng, S. Singh, Oxidative stress-mediated genotoxic effect of zinc oxide nanoparticles on Deinococcus radiodurans, 3 Biotech 10 (2020) 66.
[21] B. Ahmed, A. Hashmi, M.S. Khan, J. Musarrat, ROS mediated destruction of cell membrane, growth and biofilms of human bacterial pathogens by stable metallic AgNPs functionalized from bell pepper extract and quercetin, Adv. Powder Technol. 29 (2018) 1601–1616.
[22] H.M. Yadav, J.S. Kim, S.H. Pawar, Developments in photocatalytic antibacterial activity of nano TiO_2: a review, Kor. J. Chem. Eng. 33 (2016) 1989–1998.
[23] Y.F. Chen, X.N. Tang, X. Gao, B. Zhang, Y. Luo, X.Y. Yao, Antimicrobial property and photocatalytic antibacterial mechanism of the TiO_2-doped SiO_2 hybrid materials under ultraviolet-light irradiation and visible-light irradiation, Ceram. Int. 45 (2019) 15505–15513.
[24] S.J. Jiang, K.L. Lin, M. Cai, ZnO nanomaterials: current advancements in antibacterial mechanisms and applications, Front. Chem. 8 (2020) 580.
[25] M.A. Quinteros, V.C. Aristizabal, P.R. Dalmasso, M.G. Paraje, P.L. Paez, Oxidative stress generation of silver nanoparticles in three bacterial genera and its relationship with the antimicrobial activity, Toxicol. Vitro 36 (2016) 216–223.
[26] M.J. Piao, K.A. Kang, I.K. Lee, H.S. Kim, S. Kim, J.Y. Choi, J. Choi, J.W. Hyun, Silver nanoparticles induce oxidative cell damage in human liver cells through inhibition of reduced glutathione and induction of mitochondria-involved apoptosis, Toxicol. Lett. 201 (2011) 92–100.
[27] L.R. Bernstein, Mechanisms of therapeutic activity for gallium, Pharmacol. Rev. 50 (1998) 665–682.
[28] P.L. Carver, The battle for iron between humans and microbes, Curr. Med. Chem. 25 (2018) 85–96.
[29] R. Garcia-Contreras, E. Lira-Silva, R. Jasso-Chavez, I.L. Hernandez-Gonzalez, T. Maeda, T. Hashimoto, F.C. Boogerd, L.L. Sheng, T.K. Wood, R. Moreno-Sanchez, Isolation and characterization of gallium resistant Pseudomonas aeruginosa mutants, Int. J. Med. Microbiol. 303 (2013) 574–582.
[30] L.C.S. Antunes, F. Imperi, F. Minandri, P. Visca, In vitro and in vivo antimicrobial activities of gallium nitrate against multidrug-resistant acinetobacter baumannii, Antimicrob. Agents Chemother. 56 (2012) 5961–5970.
[31] N. Kircheva, T. Dudev, Competition between abiogenic and biogenic metal cations in biological systems: mechanisms of gallium's anticancer and antibacterial effect, J. Inorg. Biochem. 214 (2021), 111309.
[32] M.G. Thompson, V. Truong-Le, Y.A. Alamneh, C.C. Black, J. Anderl, C.L. Honnold, R.L. Pavlicek, R. Abu-Taleb, M.C. Wise, E.R. Hall, E.J. Wagar, E. Patzer, D. V. Zurawski, Evaluation of gallium citrate formulations against a multidrug-resistant strain of Klebsiella pneumoniae in a murine wound model of infection, Antimicrob. Agents Chemother. 59 (2015) 6484–6493.
[33] C.H. Goss, Y. Kaneko, L. Khuu, G.D. Anderson, S. Ravishankar, M.L. Aitken, N. Lechtzin, G. Zhou, D.M. Czyz, K. McLean, O. Olakanmi, H.A. Shuman, M. Teresi, E. Wilhelm, E. Caldwell, S.J. Salipante, D.B. Hornick, R.J. Siehnel, L. Becker, B.E. Britigan, P.K. Singh, Gallium disrupts bacterial iron metabolism and has therapeutic effects in mice and humans with lung infections, Sci. Transl. Med. 10 (2018), eaat7520.
[34] O. Olakanmi, B.E. Britigan, L.S. Schlesinger, Gallium disrupts iron metabolism of mycobacteria residing within human macrophages, Infect. Immun. 68 (2000) 5619–5627.
[35] I. Stojiljkovic, B.D. Evavold, V. Kumar, Antimicrobial properties of porphyrins, Expet Opin. Invest. Drugs 10 (2001) 309–320.
[36] G. Ciobanu, A. Maria Bargan, C. Luca, New cerium(IV)-substituted hydroxyapatite nanoparticles: preparation and characterization, Ceram. Int. 41 (2015) 12192–12201.
[37] H.M. Jing, X.Q. Wu, Y.Q. Liu, M.Q. Lü, K. Yang, Z.M. Yao, Antibacterial properties of cerium-bearing stainless steel, J. Rare Earths (2006) 223–226.
[38] A. Thill, O. Zeyons, O. Spalla, F. Chauvat, J. Rose, M. Auffan, A.M. Flank, Cytotoxicity of CeO_2 nanoparticles for Escherichia coli. Physico-chemical insight of the cytotoxicity mechanism, Environ. Sci. Technol. 40 (2006) 6151–6156.
[39] R.D. Shannon, Revised effective ionic radii and systematic studies of interatomic distances in halides and chalcogenides, Acta Crystallogr. A: Found. Adv. 32 (1976) 751–767.
[40] O. Zeyons, A. Thill, F. Chauvat, N. Menguy, C. Cassier-Chauvat, C. Orear, J. Daraspe, M. Auffan, J. Rose, O. Spalla, Direct and indirect CeO_2 nanoparticles toxicity for Escherichia coli and Synechocystis, Nanotoxicology 3 (2009) 284–295.
[41] M. Mamunur Rashid, B. Tomšič, B. Simončič, I. Jerman, D. Štular, M. Zorc, Sustainable and cost-effective functionalization of textile surfaces with Ag-doped TiO_2/polysiloxane hybrid nanocomposite for UV protection, antibacterial and self-cleaning properties, Appl. Surf. Sci. 595 (2022), 153521.
[42] P.A. Nguyen, H.P. Phan, T. Dang-Bao, V. Nguyen, N.L. Duong, X.T. Huynh, P.P. T. Vo, T.Y.L. Pham, T.N.Q. Bui, T. Nguyen, Sunlight irradiation-assisted green synthesis, characteristics and antibacterial activity of silver nanoparticles using the leaf extract of Jasminum subtriplinerve Blume, J. Plant Biochem. Biotechnol. 31 (2022) 202–205.
[43] H.Q. Yin, R. Langford, R.E. Burrell, Comparative evaluation of the antimicrobial activity of ACTICOAT* antimicrobial barrier dressing, J. Burn Care Rehabil. 20 (1999) 195–200.
[44] M. Tiwari, K. Narayanan, M.B. Thakar, H.V. Jagani, J. Venkata Rao, Biosynthesis and wound healing activity of copper nanoparticles, IET Nanobiotechnol. 8 (2014) 230–237.
[45] H. Qamar, S. Rehman, D.K. Chauhan, A.K. Tiwari, V. Upmanyu, Green synthesis, characterization and antimicrobial activity of copper oxide nanomaterial derived from momordica charantia, Int. J. Nanomed. 15 (2020) 2541–2553.
[46] E. Saebnoori, N. Koupaei, S.A.H. Tabrizi, The solution plasma synthesis, characterisation, and antibacterial activities of dispersed CuO nanoparticles, Mater. Technol. 37 (2021) 1220–1229.
[47] P. Pomastowski, A. Krol-Gorniak, V. Railean-Plugaru, B. Buszewski, Zinc oxide nanocomposites-extracellular synthesis, physicochemical characterization and antibacterial potential, Materials 13 (2020) 4347.
[48] S. Karthik, P. Siva, K.S. Balu, R. Suriyaprabha, V. Rajendran, M. Maaza, Acalypha indica-mediated green synthesis of ZnO nanostructures under differential thermal treatment: effect on textile coating, hydrophobicity, UV resistance, and antibacterial activity, Adv. Powder Technol. 28 (2017) 3184–3194.
[49] X. Zhu, D. Wu, W. Wang, F. Tan, P.K. Wong, X. Wang, X. Qiu, X. Qiao, Highly effective antibacterial activity and synergistic effect of Ag-MgO nanocomposite against Escherichia coli, J. Alloys Compd. 684 (2016) 282–290.
[50] N. Ciacotich, R.U. Din, J.J. Sloth, P. Moller, L. Gram, An electroplated copper-silver alloy as antibacterial coating on stainless steel, Surf. Coat. Technol. 345 (2018) 96–104.
[51] J.A. Garza-Cervantes, A. Chavez-Reyes, E.C. Castillo, G. Garcia-Rivas, O. A. Ortega-Rivera, E. Salinas, M. Ortiz-Martinez, S.L. Gomez-Flores, J.A. Pena-Martinez, A. Pepi-Molina, M.T. Trevino-Gonzalez, X. Zarate, M.E. Cantu-Cardenas, C.E. Escarcega-Gonzalez, J.R. Morones-Ramirez, Synergistic antimicrobial effects of silver/transition-metal combinatorial treatments, Sci. Rep. 7 (2017) 903.
[52] G. Naz, M. Shabbir, M. Ramzan, B.U. Haq, M. Arshad, M.B. Tahir, M. Hasan, R. Ahmed, Synergistic effect of Cu_x/Mg_x and $Zn_{1-x}O$ for enhanced photocatalytic degradation and antibacterial activity, Phys. B 624 (2022), 413396.
[53] D. Hong, G. Cao, J. Qu, Y. Deng, J. Tang, Antibacterial activity of Cu_2O and Ag co-modified rice grains-like ZnO nanocomposites, J. Mater. Sci. Technol. 34 (2018) 2359–2367.
[54] H. Li, X.N. Tang, B. Zhang, C.P. Mao, Y.L. Zhao, D. Zhang, Preparation, characterisation and optimisation of zinc-praseodymium inorganic antibacterial material through response surface methodology, Mater. Technol. 32 (2017) 65–71.
[55] M.M. Jiang, B. Zhang, X.N. Tang, Q.L. Liu, S.L. Tian, Preparation and characterization of hybrid antimicrobial materials based on Zn-Lu composites, J. Mater. Sci. 53 (2018) 14922–14932.
[56] S. Yang, Y. Nie, B. Zhang, X. Tang, H. Mao, Construction of Er-doped ZnO/SiO_2 composites with enhanced antimicrobial properties and analysis of antibacterial mechanism, Ceram. Int. 46 (2020) 20932–20942.
[57] W. Raza, S.M. Faisal, M. Owais, D. Bahnemann, M. Muneer, Facile fabrication of highly efficient modified ZnO photocatalyst with enhanced photocatalytic, antibacterial and anticancer activity, RSC Adv. 6 (2016) 78335–78350.
[58] N. Gao, J.S. Liang, J.P. Meng, X.Q. Ou, Effects of rare earth elements on photocatalytic antibacterial properties of nanometer TiO_2 powders, J. Rare Earths 22 (2004) 173–175.
[59] S. Ramya, S.D.R. Nithila, R.P. George, D.N.G. Krishna, C. Thinaharan, U. K. Mudali, Antibacterial studies on Eu-Ag codoped TiO_2 surfaces, Ceram. Int. 39 (2013) 1695–1705.
[60] D.M. Tobaldi, L. Lajaunie, M.L. Haro, R.A.S. Ferreira, M. Leoni, M.P. Seabra, J. J. Calvino, L.D. Carlos, J.A. Labrincha, Synergy of neodymium and copper for fast and reversible visible-light promoted photochromism, and photocatalysis, in Cu/Nd-TiO_2 nanoparticles, ACS Appl. Energy Mater. 2 (2019) 3237–3252.

[61] Y. Qiao, Z. Zhai, L. Chen, H. Liu, Cytocompatible 3D chitosan/hydroxyapatite composites endowed with antibacterial properties: toward a self-sterilized bone tissue engineering scaffold, Sci. Bull. 60 (2015) 1193–1202.
[62] Y.-E. Choe, Y.-J. Kim, S.-J. Jeon, J.-Y. Ahn, J.-H. Park, K. Dashnyam, N. Mandakhbayar, J.C. Knowles, H.-W. Kim, S.-K. Jun, J.-H. Lee, H.-H. Lee, Investigating the mechanophysical and biological characteristics of therapeutic dental cement incorporating copper doped bioglass nanoparticles, Dent. Mater. 38 (2022) 363–375.
[63] M.A. Nazeer, E. Yilgor, I. Yilgor, Intercalated chitosan/hydroxyapatite nanocomposites: promising materials for bone tissue engineering applications, Carbohydr. Polym. 175 (2017) 38–46.
[64] W.X. Li, D. Wang, W. Yang, Y. Song, Compressive mechanical properties and microstructure of PVA-HA hydrogels for cartilage repair, RSC Adv. 6 (2016) 20166–20172.
[65] A. Tampieri, T. D'Alessandro, M. Sandri, S. Sprio, E. Landi, L. Bertinetti, S. Panseri, G. Pepponi, J. Goettlicher, M. Banobre-Lopez, J. Rivas, Intrinsic magnetism and hyperthermia in bioactive Fe-doped hydroxyapatite, Acta Biomater. 8 (2012) 843–851.
[66] J.R. Wang, X. Gong, J. Hai, T.R. Li, Synthesis of silver-hydroxyapatite composite with improved antibacterial properties, Vacuum 152 (2018) 132–137.
[67] C. Fu, X.F. Zhang, K. Savino, P. Gabrys, Y. Gao, W. Chaimayo, B.L. Miller, M. Z. Yates, Antimicrobial silver-hydroxyapatite composite coatings through two-stage electrochemical synthesis, Surf. Coat. Technol. 301 (2016) 13–19.
[68] A. Jacobs, M. Gaulier, A. Duval, G. Renaudin, Silver doping mechanism in bioceramics-from Ag^{+}:Doped HAp to Ag degrees/BCP nanocomposite, Crystals 9 (2019) 326.
[69] N.O. Martínez-Gracida, S.C. Esparza-González, N.A. Castillo-Martínez, A. Serrano-Medina, I. Olivas-Armendariz, L.G. Campos-Múzquiz, E.M. Múzquiz-Ramos, Synergism in novel silver-copper/hydroxyapatite composites for increased antibacterial activity and biocompatibility, Ceram. Int. 46 (2020) 20215–20225.
[70] M. Riaz, R. Zia, A. Ijaz, T. Hussain, M. Mohsin, A. Malik, Synthesis of monophasic Ag doped hydroxyapatite and evaluation of antibacterial activity, Mater. Sci. Eng., C 90 (2018) 308–313.
[71] M. Koizhaiganova, I. Yasa, G. Gulumser, Characterization and antimicrobial activity of silver doped hydroxyapatite obtained by the microwave method, Mater Sci-Medzg 22 (2016) 403–408.
[72] A. Bhattacharjee, A. Gupta, M. Verma, P.A. Murugan, P. Sengupta, S. Matheshwara, I. Manna, K. Balani, Site-specific antibacterial efficacy and cyto/hemo-compatibility of zinc substituted hydroxyapatite, Ceram. Int. 45 (2019) 12225–12233.
[73] G. Karunakaran, E.B. Cho, G.S. Kumar, E. Kolesnikov, G. Janarthanan, M. M. Pillai, S. Rajendran, S. Boobalan, K.G. Sudha, M.P. Rajeshkumar, Mesoporous Mg-doped hydroxyapatite nanorods prepared from bio-waste blue mussel shells for implant applications, Ceram. Int. 46 (2020) 28514–28527.
[74] B. Priyadarshini, U. Anjaneyulu, U. Vijayalakshmi, Preparation and characterization of sol-gel derived Ce^{4+} doped hydroxyapatite and its in vitro biological evaluations for orthopedic applications, Mater. Des. 119 (2017) 446–455.
[75] B.K.S. Kumar, M. Jagannatham, B. Venkateswarlu, R. Dumpala, B.R. Sunil, Synthesis, characterization, and antimicrobial properties of strontium-substituted hydroxyapatite, J. Australas. Ceram. Soc. 57 (2021) 195–204.
[76] H.Q. Zhang, C.P. Zhao, J. Wen, X.Y. Li, L.W. Fu, Synthesis and structural characteristics of magnesium and zinc doped hydroxyapatite whiskers, Ceram. Silik. 61 (2017) 244–249.
[77] I.R. Gibson, W. Bonfield, Preparation and characterization of magnesium/carbonate co-substituted hydroxyapatites, J. Mater. Sci. Mater. Med. 13 (2002) 685–693.
[78] L.L. Hench, R.J. Splinter, W.C. Allen, T.K. Greenlee, Bonding mechanisms at the interface of ceramic prosthetic materials, J. Biomed. Mater. Res. 5 (1971) 117–141.
[79] Y.C. Chiang, Y.C. Wang, J.C. Kung, C.J. Shih, Antibacterial silver-containing mesoporous bioglass as a dentin remineralization agent in a microorganism-challenged environment, J. Dent. 106 (2021), 103563.
[80] R.L. Siqueira, P.F.S. Alves, T.D. Moraes, L.A. Casemiro, S.N. da Silva, O. Peitl, C. H.G. Martins, E.D. Zanotto, Cation-doped bioactive ceramics: in vitro bioactivity and effect against bacteria of the oral cavity, Ceram. Int. 45 (2019) 9231–9244.
[81] A.A.I. Fooladi, H.M. Hosseini, F. Hafezi, F. Hosseinnejad, M.R. Nourani, Sol-gel-derived bioactive glass containing SiO_2-MgO-CaO-P_2O_5 as an antibacterial scaffold, J. Biomed. Mater. Res., Part A 101 (2013) 1582–1587.
[82] J.V. Rau, M. Curcio, M.G. Raucci, K. Barbaro, I. Fasolino, R. Teghil, L. Ambrosio, A. De Bonis, A.R. Boccaccini, Cu-releasing bioactive glass coatings and their in vitro properties, ACS Appl. Mater. Interfaces 11 (2019) 5812–5820.
[83] E. Munukka, O. Lepparanta, M. Korkeamaki, M. Vaahtio, T. Peltola, D. Zhang, L. Hupa, H. Ylanen, J.I. Salonen, M.K. Viljanen, E. Eerola, Bactericidal effects of bioactive glasses on clinically important aerobic bacteria, J. Mater. Sci. Mater. Med. 19 (2008) 27–32.
[84] N. Lindfors, J. Geurts, L. Drago, J.J. Arts, V. Juutilainen, P. Hyvonen, A.J. Suda, A. Domenico, S. Artiaco, C. Alizadeh, A. Brychcy, J. Bialecki, C.L. Romano, Antibacterial bioactive glass, S53P4, for chronic bone infections - a multinational study, in: L. Drago (Ed.), A Modern Approach to Biofilm-Related Orthopaedic Implant Infections: Advances in Microbiology, vol. 5, Infectious Diseases and Public Health, 2017, pp. 81–92.
[85] E.J. Ryan, A.J. Ryan, A. Gonzalez-Vazquez, A. Philippart, F.E. Ciraldo, C. Hobbs, V. Nicolosi, A.R. Boccaccini, C.J. Kearney, F.J. O'Brien, Collagen scaffolds functionalised with copper-eluting bioactive glass reduce infection and enhance osteogenesis and angiogenesis both in vitro and in vivo, Biomaterials 197 (2019) 405–416.
[86] V. Anand, K.J. Singh, K. Kaur, Evaluation of zinc and magnesium doped 45S5 mesoporous bioactive glass system for the growth of hydroxyl apatite layer, J. Non-Cryst. Solids 406 (2014) 88–94.
[87] J. Cui, Y. Shao, H. Zhang, H. Zhang, J. Zhu, Development of a novel silver ions-nanosilver complementary composite as antimicrobial additive for powder coating, Chem. Eng. J. 420 (2021), 127633.
[88] Y. Jing, B. Mu, M. Zhang, L. Wang, H. Zhong, X. Liu, A. Wang, Zinc-loaded palygorskite nanocomposites for catheter coating with excellent antibacterial and anti-biofilm properties, Colloids Surf. Physicochem. Eng. Aspects 600 (2020), 124965.
[89] R. Tekin, N. Bac, Antimicrobial behavior of ion-exchanged zeolite X containing fragrance, Microporous Mesoporous Mater. 234 (2016) 55–60.
[90] F. Collins, A. Rozhkovskaya, J.G. Outram, G.J. Millar, A critical review of waste resources, synthesis, and applications for Zeolite LTA, Microporous Mesoporous Mater. 291 (2020), 109667.
[91] M. Li, G. Li, J. Jiang, Y. Tao, K.C. Mai, Preparation, antimicrobial, crystallization and mechanical properties of nano-ZnO-supported zeolite filled polypropylene random copolymer composites, Compos. Sci. Technol. 81 (2013) 30–36.
[92] Y. Inoue, M. Kogure, K.I. Matsumoto, H. Hamashima, M. Tsukada, K. Endo, T. Tanaka, Light irradiation is a factor in the bactericidal activity of silver-loaded zeolite, Chem. Pharm. Bull. (Tokyo) 56 (2008) 692–694.
[93] A.A. Alswat, M. Bin Ahmad, M.Z. Hussein, N.A. Ibrahim, T.A. Saleh, Copper oxide nanoparticles-loaded zeolite and its characteristics and antibacterial activities, J. Mater. Sci. Technol. 33 (2017) 889–896.
[94] M.M. Salim, N. Malek, Characterization and antibacterial activity of silver exchanged regenerated NaY zeolite from surfactant-modified NaY zeolite, Mater. Sci. Eng., C 59 (2016) 70–77.
[95] S.A.M. Hanim, N. Malek, Z. Ibrahim, Amine-functionalized, silver-exchanged zeolite NaY: preparation, characterization and antibacterial activity, Appl. Surf. Sci. 360 (2016) 121–130.
[96] M. Li, L.J. Wu, Z.S. Zhang, K.C. Mai, Preparation of ZnO-supported 13X zeolite particles and their antimicrobial mechanism, J. Mater. Res. 32 (2017) 4232–4240.
[97] X.X. Ma, Y.Y. Pei, Y.L. Ma, T. Pu, Y. Lei, Antibacterial activity of Cu^{2+}-ZnO-modified 13X zeolite against E.coli and S.aureus, J. Wuhan Univ. Technol.-Materials Sci. Ed. 34 (2019) 481–486.
[98] S. Zavareh, Z. Farrokhzad, F. Darvishi, Modification of zeolite 4A for use as an adsorbent for glyphosate and as an antibacterial agent for water, Ecotoxicol. Environ. Saf. 155 (2018) 1–8.
[99] J.J. Shao, L.L. Wang, X. Wang, J.J. Ma, Enhancing microbial management and shelf life of shrimp Penaeus vannamei by using nanoparticles of metallic oxides as an alternate active packaging tool to synthetic chemicals, Food Packag. Shelf Life 28 (2021), 100652.
[100] X.S. Hu, J. Bai, C.P. Li, H.O. Liang, W.Y. Sun, Silver-based 4A zeolite composite catalyst for styrene epoxidation by one-pot hydrothermal synthesis, Eur. J. Inorg. Chem. (2015) 3758–3763.
[101] S. Abed, H.R. Bakhsheshi-Rad, H. Yaghoubi, L.Q. Ning, A. Sadeghianmaryan, X. B. Chen, Antibacterial activities of zeolite/silver-graphene oxide nanocomposite in bone implants, Mater. Technol. 36 (2021) 660–669.
[102] P. Dutta, B. Wang, Zeolite-supported silver as antimicrobial agents, Coord. Chem. Rev. 383 (2019) 1–29.
[103] S.J. Chen, J. Popovich, N. Iannuzo, S.E. Haydel, D.K. Seo, Silver-ion-Exchanged nanostructured zeolite X as antibacterial agent with superior ion release kinetics and efficacy against methicillin-resistant Staphylococcus aureus, ACS Appl. Mater. Interfaces 9 (2017) 39271–39282.
[104] Z.U. Iyigundogdu, S. Demirci, N. Bac, F. Sahin, Development of durable antimicrobial surfaces containing silver- and zinc-ion-exchanged zeolites, Turk. J. Biol. 38 (2014) 420–427.
[105] M.I. Carretero, Clay minerals and their beneficial effects upon human health, A review, Appl. Clay Sci. 21 (2002) 155–163.
[106] S.K. Jou, N. Malek, Characterization and antibacterial activity of chlorhexidine loaded silver-kaolinite, Appl. Clay Sci. 127 (2016) 1–9.
[107] C.F. Gomes, J.H. Gomes, E.F. da Silva, Bacteriostatic and bactericidal clays: an overview, Environ. Geochem. Health 42 (2020) 3507–3527.
[108] K. Malachova, P. Praus, Z. Rybkova, O. Kozak, Antibacterial and antifungal activities of silver, copper and zinc montmorillonites, Appl. Clay Sci. 53 (2011) 642–645.
[109] J. Song, Y.L. Li, C.H. Hu, Effects of copper-exchanged montmorillonite, as alternative to antibiotic, on diarrhea, intestinal permeability and proinflammatory cytokine of weanling pigs, Appl. Clay Sci. 77–78 (2013) 52–55.
[110] C.C. Otto, J.L. Koehl, D. Solanky, S.E. Haydel, Metal ions, not metal-catalyzed oxidative stress, cause clay leachate antibacterial activity, PLoS One 9 (2014), e115172.
[111] M. Sprynskyy, H. Sokol, K. Rafinska, W. Brzozowska, V. Railean-Plugar, P. Pomastowski, B. Buszewski, Preparation of AgNPs/saponite nanocomposites without reduction agents and study of its antibacterial activity, Colloids Surf., B 180 (2019) 457–465.
[112] H.L. Su, C.C. Chou, D.J. Hung, S.H. Lin, I.C. Pao, J.H. Lin, F.L. Huang, R.X. Dong, J.J. Lin, The disruption of bacterial membrane integrity through ROS generation induced by nanohybrids of silver and clay, Biomaterials 30 (2009) 5979–5987.
[113] S.M. Magana, P. Quintana, D.H. Aguilar, J.A. Toledo, C. Angeles-Chavez, M. A. Cortes, L. Leon, Y. Freile-Pelegrin, T. Lopez, R.M.T. Sanchez, Antibacterial activity of montmorillonites modified with silver, J. Mol. Catal. Chem. 281 (2008) 192–199.

[114] S.Z. Tan, K.H. Zhang, L.L. Zhang, Y.S. Xie, Y.L. Liu, Preparation and characterization of the antibacterial $Zn^{(2+)}$ or/and $Ce^{(3+)}$ loaded montmorillonites, Chin. J. Chem. 26 (2008) 865–869.

[115] C.H. Hu, Z.R. Xu, M.S. Xia, Antibacterial effect of Cu^{2+}-exchanged montmorillonite on Aeromonas hydrophila and discussion on its mechanism, Vet. Microbiol. 109 (2005) 83–88.

[116] M. Isah, M.H. Asraf, N. Malek, K. Jemon, N.S. Sani, M.S. Muhammad, M.F. A. Wahab, M.A.R. Saidin, Preparation and characterization of chlorhexidine modified zinc-kaolinite and its antibacterial activity against bacteria isolated from water vending machine, J. Environ. Chem. Eng. 8 (2020), 103545.

[117] N. Malek, S.A. Ishak, M.R.A. Kadir, Antibacterial activity of copper and CTAB modified clays against Pseudomonas aeruginosa, Adv. Mater. Res. (2012) 178–182.

[118] N. Saad, N. Malek, C.S. Chong, Antimicrobial activity of copper kaolinite and surfactant modified copper kaolinite against gram positive and gram negative bacteria, Jurnal Teknologi 78 (2016) 127–132.

[119] B. Benli, C. Yalm, The influence of silver and copper ions on the antibacterial activity and local electrical properties of single sepiolite fiber: a conductive atomic force microscopy (C-AFM) study, Appl. Clay Sci. 146 (2017) 449–456.

[120] A. Roy, B.S. Butola, M. Joshi, Synthesis, characterization and antibacterial properties of novel nano-silver loaded acid activated montmorillonite, Appl. Clay Sci. 146 (2017) 278–285.

[121] Z. Shu, Y. Zhang, Q. Yang, H.M. Yang, Halloysite nanotubes supported Ag and ZnO nanoparticles with synergistically enhanced antibacterial activity, Nanoscale Res. Lett. 12 (2017) 135.

[122] Y. Guo, M. Zhang, C. Duan, X. Dong, Study and application of inorganic antibacterial materials, Yunnan Huagong 47 (2020) 18–20.

[123] M. Cloutier, D. Mantovani, F. Rosei, Antibacterial coatings: challenges, perspectives, and opportunities, Trends Biotechnol. 33 (2015) 637–652.

[124] M. Oliverius, J. Drozd, P. Bratka, A. Whitley, B.M. Duchonova, R. Gurlich, A new silver dressing, StopBac, used in the prevention of surgical site infections, Int. Wound J. 19 (2022) 29–35.

[125] C.C. Guo, W.D. Cui, X.W. Wang, X.X. Lu, L.L. Zhang, X.Y. Li, W. Li, W.B. Zhang, J. L. Chen, Poly-L-lysine/Sodium alginate coating loading nanosilver for improving the antibacterial effect and inducing mineralization of dental implants, ACS Omega 5 (2020) 10562–10571.

[126] B. Li, X.Y. Liu, C. Cao, F.H. Meng, Y.Q. Dong, T. Cui, C.X. Ding, Preparation and antibacterial effect of plasma sprayed wollastonite coatings loading silver, Appl. Surf. Sci. 255 (2008) 452–454.

[127] M.J. Fu, Y.J. Liang, X. Lv, C.N. Li, Y.Y. Yang, P.Y. Yuan, X. Ding, Recent advances in hydrogel-based anti-infective coatings, J. Mater. Sci. Technol. 85 (2021) 169–183.

[128] H. Chouirfa, H. Bouloussa, V. Migonney, C. Falentin-Daudre, Review of titanium surface modification techniques and coatings for antibacterial applications, Acta Biomater. 83 (2019) 37–54.

[129] H. Zhu, Z.G. Guo, W.M. Liu, Adhesion behaviors on superhydrophobic surfaces, Chem. Commun. 50 (2014) 3900–3913.

[130] D. Campoccia, L. Montanaro, C.R. Arciola, A review of the biomaterials technologies for infection-resistant surfaces, Biomaterials 34 (2013) 8533–8554.

[131] J. Seyfi, M. Panahi-Sarmad, A. OraeiGhodousi, V. Goodarzi, H.A. Khonakdar, A. Asefnejad, S. Shojaei, Antibacterial superhydrophobic polyvinyl chloride surfaces via the improved phase separation process using silver phosphate nanoparticles, Colloids Surf., B 183 (2019), 110438.

[132] Y.L. Zhan, S.R. Yu, A. Amirfazli, A.R. Siddiqui, W. Li, Recent advances in antibacterial superhydrophobic coatings, Adv. Eng. Mater. 24 (2022), 2101053.

[133] S. Varghese, S.O. ElFakhri, D.W. Sheel, P. Sheel, F.J.E. Bolton, H.A. Foster, Antimicrobial activity of novel nanostructured Cu-SiO_2 coatings prepared by chemical vapour deposition against hospital related pathogens, Amb. Express 3 (2013) 53.

[134] I.A. Hassan, I.P. Parkin, S.P. Nair, C.J. Carmalt, Antimicrobial activity of copper and copper(I) oxide thin films deposited via aerosol-assisted CVD, J. Mater. Chem. B 2 (2014) 2855–2860.

[135] E. Ozkan, C.C. Crick, A. Taylor, E. Allan, I.P. Parkin, Copper-based water repellent and antibacterial coatings by aerosol assisted chemical vapour deposition, Chem. Sci. 7 (2016) 5126–5131.

[136] S. Gerullis, A. Pfuch, S. Spange, F. Kettner, K. Plaschkies, B. Kuzun, P. V. Kosmachev, G.G. Volokitin, B. Grunler, Thin antimicrobial silver, copper or zinc containing SiO_x films on wood polymer composites (WPC) applied by atmospheric pressure plasma chemical vapour deposition (APCVD) and sol-gel technology, Eur. J. Wood Wood Prod. 76 (2018) 229–241.

[137] M. Zeiger, M. Solioz, H. Edongue, E. Arzt, A.S. Schneider, Surface structure influences contact killing of bacteria by copper, MicrobiologyOpen 3 (2014) 327–332.

[138] S.Y. Li, Y. Liu, Z.Z. Tian, X. Liu, Z.W. Han, L.Q. Ren, Biomimetic superhydrophobic and antibacterial stainless-steel mesh via double-potentiostatic electrodeposition and modification, Surf. Coat. Technol. 403 (2020), 126355.

[139] W. Hong, M.W. Meng, Q.Y. Liu, D.D. Gao, C.Y. Kang, S.Y. Huang, Z.M. Zhou, C. Q. Chen, Antibacterial and photocatalytic properties of Cu_2O/ZnO composite film synthesized by electrodeposition, Res. Chem. Intermed. 43 (2017) 2517–2528.

[140] C. Balagna, R. Francese, S. Perero, D. Lembo, M. Ferraris, Nanostructured composite coating endowed with antiviral activity against human respiratory viruses deposited on fibre-based air filters, Surf. Coat. Technol. 409 (2021), 126873.

[141] C. Balagna, S. Perero, E. Percivalle, E.V. Nepita, M. Ferraris, Virucidal effect against coronavirus SARS-CoV-2 of a silver nanocluster/silica composite sputtered coating, Open Ceramics 1 (2020), 100006.

[142] M. Wasim, M.R. Khan, M. Mushtaq, A. Naeem, M.C. Han, Q.F. Wei, Surface modification of bacterial cellulose by copper and zinc oxide sputter coating for UV-Resistance/Antistatic/Antibacterial characteristics, Coatings 10 (2020) 364.

[143] M. Anwar, Z.N. Kayani, A. Hassan, An insight of physical and antibacterial properties of Au-doped ZnO dip coated thin films, Opt. Mater. 118 (2021), 111276.

[144] M. Maulidiyah, P.E. Susilowati, N.K. Mudhafar, L.A. Salim, D. Wibowo, M. Z. Muzakkar, I. Irwan, Z. Arham, M. Nurdin, Photo-inactivation Staphylococcus aureus by using formulation of Mn-N-TiO_2 composite coated wall paint, Biointerface Res. Appl. Chem. 12 (2022) 1628–1637.

[145] Y.C. Li, S.T. Xie, D. Xu, G. Shu, X.X. Wang, Antibacterial activity of ZnO quantum dots and its protective effects of chicks infected with Salmonella pullorum, Nanotechnology 32 (2021), 505104.

[146] O. Sharifahmadian, H.R. Salimijazi, M.H. Fathi, J. Mostaghimi, L. Pershin, Study of the antibacterial behavior of wire arc sprayed copper coatings, J. Therm. Spray Technol. 22 (2013) 371–379.

[147] M.T. Tsai, Y.Y. Chang, H.L. Huang, J.T. Hsu, Y.C. Chen, A.Y.J. Wu, Characterization and antibacterial performance of bioactive Ti-Zn-O coatings deposited on titanium implants, Thin Solid Films 528 (2013) 143–150.

[148] S.F. Seyedpour, A. Rahimpour, A.A. Shamsabadi, M. Soroush, Improved performance and antifouling properties of thin-film composite polyamide membranes modified with nano-sized bactericidal graphene quantum dots for forward osmosis, Chem. Eng. Res. Des. 139 (2018) 321–334.

[149] X.J. Han, Z.M. Huang, C. Huang, Z.F. Du, H. Wang, J. Wang, C.L. He, Q.S. Wu, Preparation and characterization of electrospun polyurethane/inorganic-particles nanofibers, Polym. Compos 33 (2012) 2045–2057.

[150] A. Choi, J. Park, J. Kang, O. Jonas, D.W. Kim, H. Kim, J.W. Oh, Y.C. Kang, Surface characterization and investigation on antibacterial activity of CuZn nanofibers prepared by electrospinning, Appl. Surf. Sci. 508 (2020), 144883.

[151] S.H. Park, Y.S. Ko, S.J. Park, J.S. Lee, J. Cho, K.Y. Baek, I.T. Kim, K. Woo, J.H. Lee, Immobilization of silver nanoparticle-decorated silica particles on polyamide thin film composite membranes for antibacterial properties, J. Membr. Sci. 499 (2016) 80–91.

[152] S. Azlin-Hasim, M.C. Cruz-Romero, E. Cummins, J.P. Kerry, M.A. Morris, The potential use of a layer-by-layer strategy to develop LDPE antimicrobial films coated with silver nanoparticles for packaging applications, J. Colloid Interface Sci. 461 (2016) 239–248.

[153] Z.Y. Liu, L.B. Qi, X.C. An, C.F. Liu, Y.X. Hu, Surface engineering of thin film composite polyamide membranes with silver nanoparticles through layer-by-layer interfacial polymerization for antibacterial properties, ACS Appl. Mater. Interfaces 9 (2017) 40987–40997.

[154] T.Z. Jin, Current state of the art and recent innovations for antimicrobial food packaging, in: V.K. Juneja, H.P. Dwivedi, J.N. Sofos (Eds.), Microbial Control and Food Preservation: Theory and Practice, Springer New York, New York, NY, 2017, pp. 349–372.

[155] V.M. Rangaraj, S. Devaraju, K. Rambabu, F. Banat, V. Mittal, Silver-sepiolite (Ag-Sep) hybrid reinforced active gelatin/date waste extract (DSWE) blend composite films for food packaging application, Food Chem. 369 (2022), 130983.

[156] R. Gu, H. Yun, L.F. Chen, Q. Wang, X.J. Huang, Regenerated cellulose films with amino-terminated hyperbranched polyamic anchored nanosilver for active food packaging, ACS Appl. Bio Mater. 3 (2020) 602–610.

[157] E. Kowsalya, K. MosaChristas, P. Balashanmugam, A.T. Selvi, I.J.C. Rani, Biocompatible silver nanoparticles/poly(vinyl alcohol) electrospun nanofibers for potential antimicrobial food packaging applications, Food Packag. Shelf Life 21 (2019), 100379.

[158] M. Singh, T. Sahareen, Investigation of cellulosic packets impregnated with silver nanoparticles for enhancing shelf-life of vegetables, LWT–Food Sci. Technol. 86 (2017) 116–122.

[159] J. Deng, Q.J. Chen, Z.Y. Peng, J.H. Wang, W. Li, Q.M. Ding, Q.L. Lin, D.M. Liu, S. S. Wang, Y. Shi, Y. Liu, S.S. Feng, Nano-silver-containing polyvinyl alcohol composite film for grape fresh-keeping, Mater. Express 9 (2019) 985–992.

[160] E. Jamroz, P. Kopel, L. Juszczak, A. Kawecka, Z. Bytesnikova, V. Milosavljevic, M. Makarewicz, Development of furcellaran-gelatin films with Se-AgNPs as an active packaging system for extension of mini kiwi shelf life, Food Packag. Shelf Life 21 (2019), 100339.

[161] S. Shankar, J.W. Rhim, Preparation and characterization of agar/lignin/silver nanoparticles composite films with ultraviolet light barrier and antibacterial properties, Food Hydrocolloids 71 (2017) 76–84.

[162] H. Chambi, C. Grosso, Edible films produced with gelatin and casein cross-linked with transglutaminase, Food Res. Int. 39 (2006) 458–466.

[163] K. Shameli, M. Bin Ahmad, W. Yunus, N.A. Ibrahim, R.A. Rahman, M. Jokar, M. Darroudi, Silver/poly (lactic acid) nanocomposites: preparation, characterization, and antibacterial activity, Int. J. Nanomed. 5 (2010) 573–579.

[164] General Administration of Customs of the People's Republic of China, Customs Today, Customs Today, 2022. http://www.customs.gov.cn/customs/xwfb34/302425/index.html. (Accessed 10 April 2022).

[165] M. Zare, K. Namratha, S. Ilyas, A. Hezam, S. Mathur, K. Byrappa, Smart fortified PHBV-CS biopolymer with ZnO–Ag nanocomposites for enhanced shelf life of food packaging, ACS Appl. Mater. Interfaces 11 (2019) 48309–48320.

[166] L. Kuuliala, T. Pippuri, J. Hultman, S.M. Auvinen, K. Kolppo, T. Nieminen, M. Karp, J. Bjorkroth, J. Kuusipalo, E. Jaaskelainen, Preparation and antimicrobial characterization of silver-containing packaging materials for meat, Food Packag. Shelf Life 6 (2015) 53–60.

[167] B. Kilinc, S. Altas, G. Surengil, N. Ozdil, The development of new and alternative type of packaging for atlantic salmon (Salmo salar) fillets by producing nonwoven fabrics, J. Food Process. Preserv. 41 (2017), e12850.

[168] F.P. Mousavi, H.H. Pour, A.H. Nasab, A.A. Rajabalipour, M. Barouni, Investigation into shelf life of fresh dates and pistachios in a package modified with nano-silver, Global J. Health Sci. 8 (2015) 134–144.
[169] A. Fernandez, P. Picouet, E. Lloret, Cellulose-silver nanoparticle hybrid materials to control spoilage-related microflora in absorbent pads located in trays of fresh-cut melon, Int. J. Food Microbiol. 142 (2010) 222–228.
[170] R. Ruckerl, A. Schneider, S. Breitner, J. Cyrys, A. Peters, Health effects of particulate air pollution: a review of epidemiological evidence, Inhal. Toxicol. 23 (2011) 555–592.
[171] P.V. AshaRani, G.L.K. Mun, M.P. Hande, S. Valiyaveettil, Cytotoxicity and genotoxicity of silver nanoparticles in human cells, ACS Nano 3 (2009) 279–290.
[172] C. Greulich, J. Diendorf, J. Gessmann, T. Simon, T. Habijan, G. Eggeler, T. A. Schildhauer, M. Epple, M. Koller, Cell type-specific responses of peripheral blood mononuclear cells to silver nanoparticles, Acta Biomater. 7 (2011) 3505–3514.
[173] A. Emamifar, M. Kadivar, M. Shahedi, S. Soleimanian-Zad, Effect of nanocomposite packaging containing Ag and ZnO on inactivation of Lactobacillus plantarum in orange juice, Food Control 22 (2011) 408–413.
[174] Y. Echegoyen, C. Nerin, Nanoparticle release from nano-silver antimicrobial food containers, Food Chem. Toxicol. 62 (2013) 16–22.
[175] C. Buzea, I.I. Pacheco, K. Robbie, Nanomaterials and nanoparticles: sources and toxicity, Biointerphases 2 (2007) MR17–MR71.
[176] B.F. Zhu, C.L. Fan, C.S. Cheng, T.Q. Lan, L. Li, Y.Y. Qin, Migration kinetic of silver from polylactic acid nanocomposite film into acidic food simulant after different high-pressure food processing, J. Food Sci. 86 (2021) 2481–2490.
[177] G. Artiaga, K. Ramos, L. Ramos, C. Camara, M. Gomez-Gomez, Migration and characterisation of nanosilver from food containers by AF(4)-ICP-MS, Food Chem. 166 (2015) 76–85.
[178] H. Ahari, L.K. Lahijani, Migration of silver and copper nanoparticles from food coating, Coatings 11 (2021) 380.
[179] A.A. Becaro, F.C. Puti, A.R. Panosso, J.C. Gern, H.M. Brandao, D.S. Correa, M. D. Ferreira, Postharvest quality of fresh-cut carrots packaged in plastic films containing silver nanoparticles, Food Bioprocess Technol. 9 (2016) 637–649.
[180] J.Y. Liu, R.H. Hurt, Ion release kinetics and particle persistence in aqueous nano-silver colloids, Environ. Sci. Technol. 44 (2010) 2169–2175.
[181] F. Liu, C.Y. Hu, Q. Zhao, Y.J. Shi, H.N. Zhong, Migration of copper from nanocopper/LDPE composite films, Food Addit. Contam. Part A Chem. Anal. Control Expo. Risk Assess. 33 (2016) 1741–1749.
[182] H. Chi, J. Xue, C. Zhang, H.Y. Chen, L. Li, Y.Y. Qin, High pressure treatment for improving water vapour barrier properties of poly(lactic acid)/Ag nanocomposite films, Polymers 10 (2018) 1011.